Study of the microbial community structure in the rhizosphere of understory dwarf bamboo (*Sasa kurilensis*) in a *Betula ermanii* forest, northern Japan

Bihe Kong

A Dissertation submitted to
The Division of Bioscience,
Graduate School of Environmental Earth Science,
Hokkaido University
for the Degree of Doctor of Philosophy in
Environmental Earth Science

Contents

Summary

Understory dwarf bamboos (genus *Sasa*), which are clonal evergreen plants, are distributed widely in the boreal forests of northern Japan. Previous studies have demonstrated that *Sasa* spp. play an important role in preserving the concentrations of carbon (C) and nitrogen (N) in soil. In the current study, I compared the microbial community structures in the soil of a *Betula ermanii* boreal forest in the presence and absence of *Sasa kurilensis* to understand the relationships between understory bamboo and soil properties. The presence of understory *S. kurilensis* affected soil properties, including total C content, total N content, nitrate-N concentration, the C:N ratio, and relative soil moisture. There were also notable differences between the fungal and bacterial communities of the abundance in the presence and absence of *S. kurilensis*. The relative abundance of the fungal phylum *Ascomycota* was 13.9% in the *Sasa*-intact plot and only 0.54% in the plot without *Sasa*. Among the identified *Ascomycota* fungi, the most prevalent were members of the family *Pezizaceae*. The abundance of *Pezizaceae*, which is known to form as mycorrhizal fungi, correlated with the amount of total C in the *Sasa*-intact plot. Additionally, among the bacteria identified, the abundance of *Proteobacteria* was significantly higher in the *Sasa*-intact plot than in the *Sasa*-removed plot, whereas those of *Planctomycetes* and *Actinobacteria* were significantly lower. Furthermore, species richness analysis suggested that some

species of the bacterial phylum *Planctomycetes* has function only in the presence of *S. kurilensis*, which related to total C and N contents. The abundance of phyla *Bacteroidetes* and *Firmicutes* correlated with nitrate-N concentration or pH, and the phyla *Acidobacteria, Proteobacteria, Planctomycetes, Verrucomicrobia* and *Actinobacteria* were each strongly negatively correlated with the total C and total N contents, the ammonium-N concentration, or the C:N ratio in the *Sasa*-intact plot. The fungal phylum *Basidiomycota* closely correlated with pH. Both the abundance of phyla *Ascomycota* and *Zygomycota* were positively correlated with the total C and total N contents, the ammonium-N concentration, and the C:N ratio in the *Sasa*-intact plot, but they were negative correlated with the nitrate-N concentration in the *Sasa*-removed plot. These findings suggest that the composition of microbial communities in *S. kurilensis*'s rhizosphere soil and its soil properties in *Betula* forests are closely related, possibly because of their interactions with one other. Collectively, the presence of *S. kurilensis* affects soil properties and microbial communities in *B. ermanii* boreal forests.

Chapter 1
General Introduction

Boreal forests comprise approximately 25% of the world's forested land, and they affect the global climate by releasing large soil carbon (C) stocks (Post et al., 1982). Dwarf bamboos often dominate forest understory vegetation in Japanese boreal forests. Dwarf bamboos, belonging to the genus *Sasa*, often form dense pure stands that other species cannot invade (Takahashi et al., 2003; Tripathi et al., 2005; Tripathi et al., 2006; Ishii et al., 2008). In Hokkaido, Japan, *Sasa* spp. cover 89% (50,000 km^2) of the forested area, and the biomass of their dry weight is approximately 75 Mt (Toyooka et al., 1983). In areas with heavy snowfall, dwarf bamboo *Sasa* spp. can quickly cover forests, growing to 0.3–3 m in height, with vigorously extending rhizomes (Oshima, 1962; Suyama et al., 2000). They flower simultaneously over an extensive area on an approximately 60-year cycle and then die (Makita, 1998). After the mass flowering and deaths, *Sasa* species' populations recover from even-aged seedlings to grow to the full-developed stage (Makita, 1992; Makita et al., 1993).

Understory *Sasa* spp. play an important role in northern Japanese boreal forests. In mixed forests, dense understory *Sasa* spp. affect the regeneration of tree species, as well as overstory tree seedling growth and establishment (Nakashizuka, 1988; Kudoh et al., 1999). Moreover, understory *Sasa* spp. are relevant to boreal forest soil properties. For example, Fukuzawa et al. (2015) reported that *Sasa senanensis* (Franch. & Sav.) Rehder is a key component species that can mitigate the loss of nitrogen (N) and C from soil. The growth of Erman's birch (*Betula ermanii*

Cham.) also increases due to the increasing soil water availability after the removal of understory *Sasa* (Takahashi et al., 2003). However, little is known about the effect of *Sasa* on the dynamics and drivers for the storage of soil properties in northern Japanese boreal forests.

In nutrient-poor ecosystems, soil microbes and plants are critical mutualists that are responsible for establishing forest soil nutrients (Van Der Heijden et al., 2008). Some soil organisms such as mycorrhizae can form symbiotic associations with plant roots. Mycorrhizae are fungus and root associations, which include two common types: ectomycorrhizae (EM) and arbuscular mycorrhizae (AM). EM fungi are characterized by a dense hyphal sheath, known as the mantle, which encloses the tips of roots, as well as the hartig net that lies between the epidermal and cortical cells. EM fungi form symbiotic associations with forest tree roots, and they greatly enhance plant growth and development by improving nutrient and water availability (Duddridge et al., 1980; Oliveira et al., 2012). For AM fungi, the root tip is usually not colonized and hyphae can reach the root inner cortex to develop highly branched structures. Endophyte usually describes a fungus that lives within above-ground healthy plant tissue without causing apparent disease. In comparison, AM fungi refer to a fungus that has a mutualistic relationship with plant roots. Fukuchi et al. (2011) found that AM fungi and endophytic fungi can occur together at sites where *S. senanensis* dominates. In the mechanisms of plant-fungus interaction, hexose transporters was identified to import plant C to

the AM fungus (Schüßler et al., 2006). Nevertheless, in boreal forests, EM fungi have a greater potential than AM fungi to store soil C (Averill et al., 2014). Boreal forests act as net terrestrial C sinks, in which a large amount of C is stored in root-associated fungi (Clemmensen et al., 2013; Osman, 2013). These studies suggest that mycorrhizal fungi in forests are an important agent to store C. Bacterial communities have also been observed to coexist with fungi in mycorrhizae. Mycorrhiza helper bacteria (MHB) have been studied widely in diverse plant–fungus model systems, and had effects on store C in many herbaceous and woody plant species (Frey-Klett et al., 2007). In order to understand the effect of *Sasa* below the forest ground, it is necessary to conduct a survey of the microbial community structure in *Sasa* rhizosphere soils.

However, owing to the complexity of microbial communities in forest habitats, it is difficult to determine the species structure of soil microorganism communities under natural conditions. Tsutsumi et al. (2009) reported that the presence of *S. kurilensis* was closely correlated with the composition of methanotrophic bacterial communities. To date, no studies have investigated the entire microbial community in the rhizosphere soils of boreal forests in northern Japan where *Sasa* spp. are typical understory plants. Fortunately, rapid advances in molecular ecological approaches have made it possible to analyze entire microbial communities in a relatively short time. Denaturing gradient gel electrophoresis (DGGE) of polymerase chain reaction (PCR)-amplified ribosomal RNA gene

fragments has been used to study microbial ecology (Muyzer et al., 1993). In DGGE, DNA fragments of the same length, but with different sequences, can be separated based on the decreased electrophoretic mobility of the denatured double-stranded DNA molecule in polyacrylamide gels due to differences in the melting temperatures of the DNA fragments; thus, fragments with different sequences will migrate to different positions in a gel (Muyzer and Smalla, 1998). Next-generation sequencing (NGS) methods, especially the Illumina sequencing method, are widely used, and they are indispensable tools for environmental DNA research (Wang et al., 2012; Schmidt et al., 2013; Hong et al., 2015). The Illumina sequencing method leverages clonal array formation and proprietary reverse terminator technology for large-scale sequencing. In addition, the Illumina MiSeq system has the advantage of allowing a higher sequencing depth compared with other NGS methods, such as 454 pyrosequencing (Caporaso et al., 2012; Schmidt et al., 2013; Uroz et al., 2013).

In the present study, I analyzed the microbial community structures of soils with or without understory *Sasa kurilensis* in a *B. ermanii* stand, and aimed to determine the relationships between the community structures and the soil physicochemical properties. The main objectives of this study were to answer the following questions: (i) what are the structures of the microbial communities in the presence and absence of *S. kurilensis*? and (ii) how are these structures related to the soil physicochemical properties?

Chapter 2
Materials and Methods

2.1 Study site

The study was conducted in the Uryu Experiment Forest of Hokkaido University (44°23′N, 142°19′E) in northern Japan. The tree layer of the forest was exclusively dominated by a birch species, *B. ermanii*, and the forest floor was densely covered with *S. kurilensis*. Two plots of 20 × 30 m were established in this forest in 1998 (Takahashi et al., 2003; Ishii et al., 2008). *Sasa kurilensis* has been removed continuously since 1998 in one plot (the *Sasa*-removed plot; SR) and left intact in the other plot (the *Sasa*-intact plot; SI). The distance between these two plots was approximately 50 m.

2.2 Microclimate

Soil temperature and moisture were monitored using TOMST thermometers (TOMST Ltd., Prague, Czech Republic) (Holec and Wild, 2011; Lexa et al., 2011; Hernandez et al., 2014). Three temperature readings (the air temperature at 10 cm above soil surface, the soil surface temperature, and the 15-cm-deep soil temperature) and soil moisture were recorded every 15 min. A TOMST thermometer measuring system was set at the center of each of three fixed circles (10 m in diameter) on a diagonal line in the two plots (Fig. 2.1)

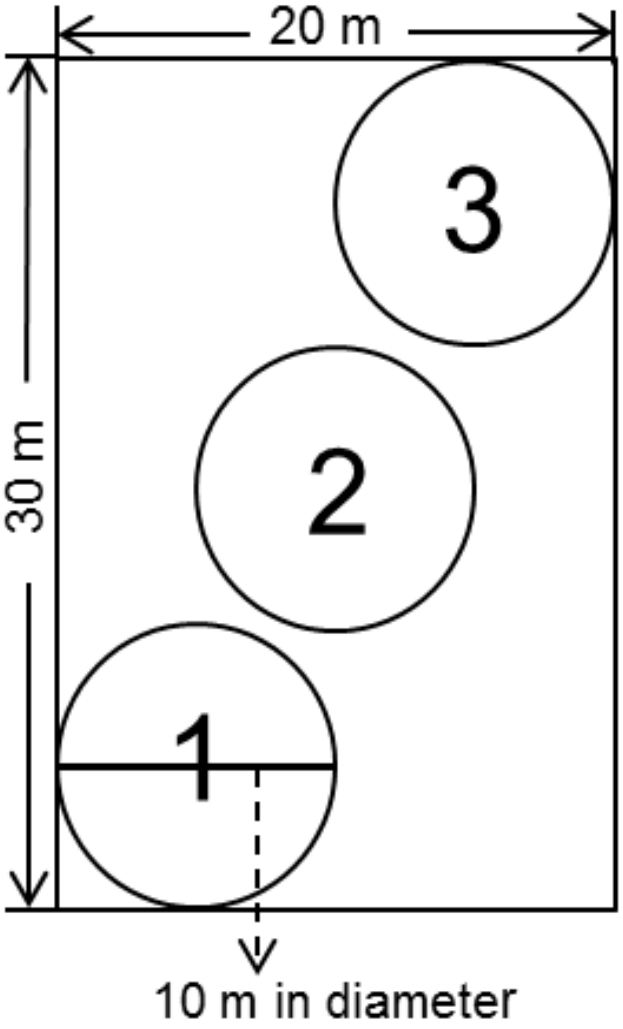

Fig. 2.1 Locations of the three sampling circles used in both study plots (*Sasa*-intact and *Sasa*-removed).

2.3 Sample collection

Soil samples were collected five times during the growing season on 23 July 2014, 1 October 2014, 3 June 2015, 4 August 2015, and 1 October 2015, avoiding the snowy season. Three soil clods (1,000 cm^3) were collected randomly at a depth

of 0–10 cm from each of three fixed circles in the two plots. In the SI plot, soil samples, including *S. kurilensis* rhizomes, were shaken vigorously to separate roots and soil that did not adhere tightly to the roots. Three replicate soil samples from each circle were mixed as one sample, packed in sterile plastic bags (Ziploc; SC Johnson Co., Racine, WI, USA), and transported to the laboratory in an ice-cooled box. After sieving through a 2-mm screen, each soil sample was divided into three parts and stored at −80°C, 4°C, or room temperature, respectively.

2.4 Soil properties

Thirty soil samples (five sampling dates × two plots × three circles) from the two plots were collected. Soil pH was measured using a glass electrode after shaking with deionized water (1:2.5 soil:water ratio) for 1 h. The total nitrogen (TN) and total carbon (TC) contents in the air-dried soil samples were measured using an automatic analyzer (C-N Corder; Yanaco, Kyoto, Japan). To measure inorganic N, fresh soil samples were mixed with deionized water (1:5 soil:water) for nitrate-N (NO_3-N) and nitrite-N (NO_2-N), and with 2 M KCl (1:10 soil:KCl) for ammonium-N (NH_4-N). The concentrations of NO_3-N and NO_2-N were measured using ion chromatography (Dionex Model ICS-1100; Thermo Fisher Scientific, Waltham, MA, USA) and ammonium using the indophenol blue method (Keeney and Nelson, 1982).

2.5 DNA extraction

The PowerSoil™ DNA Isolation Kit (MO BIO Laboratories, Solana Beach, CA, USA) was used to extract DNA from 0.25 g of fresh soil samples according to the manufacturer's instructions. The genomic DNA content of each sample was greater than 200 ng, and the DNA concentration was greater than 6 ng/μl, as determined by an analysis with a Beckman DU800 spectrophotometer (Beckman Coulter, Inc., Fullerton, CA, USA) without any evidence of degradation.

2.6 DGGE method

In the DGGE method, the DNA isolated from each sample for an analysis of the bacterial community was amplified using forward (F984GC, 5′–GC Clamp + AA CGC GAA GAA CCT TAC–3′) and reverse (R1378, 5′–CGG TGT GTA CAA GGC CCG GGA ACG–3′) primers, which yields a 433-bp amplification product (Heuer et al., 1997). PCR amplification of the 16S rRNA gene was performed by 35 cycles of 1 min of denaturation at 94°C, followed by 1 min at 63°C for primer annealing and 2 min at 72°C for primer extension, followed by a final extension step at 72°C for 10 min and cooling to 4°C (Heuer et al., 1997). For the fungal community analysis, the DNA was amplified using forward (NS1, 5′–GTA GTC ATA TGC TTG TCT C–3′) and reverse (GCFung, 5′–GC clamp + AT TCC CCG TTA CCC GTT G–3′) primers, which yields a 370-bp amplification product (May et al., 2001). PCR amplification of the 18S rRNA gene was performed by 40 cycles of 3 min of denaturation at 94°C,

followed by 1 min at 50°C for primer annealing and 3 min at 72°C for primer extension, followed by a final extension step at 72°C for 10 min and cooling to 4°C. All the PCR products were analyzed by ethidium bromide staining following electrophoresis in 1.5% (wt/vol) agarose gels.

DGGE analyses were performed using the D-GENE™ Denaturing Gel Electrophoresis System (Bio-Rad Laboratories, Hercules, CA, USA). Samples of PCR-amplified bacterial DNA (pooled from the three soil replicates) were loaded on 8% (w/v) polyacrylamide gels comprising 1× Tris-acetate-EDTA (TAE) with denaturing gradients of 40%–60% (100% denaturant corresponds to 40% formamide and 7 M urea). The gels were run at 50 V and 60 °C for 20 h, and stained in 200 ml of 1× TAE containing 20 μL of 10000× SYBR green I (Molecular Probes, Inc., Eugene, OR, USA).

2.7 NGS method

In the NGS method (Fig. 2.2), the DNA isolated from each sample was amplified using forward (Bakt_341F, 5′–CCT ACG GGN GGC WGC AG–3′) and reverse (Bakt_805R, 5′–GAC TAC HVG GGT ATC TAA TCC–3′) primers targeting the the V3-V4 region of the bacterial 16S rRNA gene (Herlemann et al., 2011). Forward (ITS3, 5′– GCA TCG ATG AAG AAC GCA GC–3′) and reverse (ITS4, 5′–TCC TCC GCT TAT TGA TAT GC–3′) primers were also used to amplify fungal internal transcribed spacer (ITS) genes (Baldwin, 1992).

Fifteen sequencing libraries were prepared from each plot with random fragmentation of the DNA samples, followed by 5′ and 3′ adapter ligation. Then, the adapter-ligated fragments were used for PCR, and the amplicons were purified from the gel according to the Illumina library preparation protocol. DNA sequencing was performed by Macrogen Inc. (Seoul, Korea) using the Illumina MiSeq platform (San Diego, CA, USA) according to the manufacturer's instructions. The sequencing library was prepared by random fragmentation of the DNA samples, followed by 5′ and 3′ adapter ligation. Then, the adapter-ligated fragments were used for PCR, and the amplicons were purified from the gel, as described in the Illumina library preparation protocols (Caporaso et al., 2012; Schmidt et al., 2013).

Raw data formatted as FASTQ were analyzed with FLASH version 1.2.11 to merge paired-end 300-bp reads from the NGS experiments (Magoč and Salzberg, 2011). The CD-HIT-OTU program (http://weizhong-lab.ucsd.edu/cd-hit-otu/) was used to identify operational taxonomic units (OTUs) (Li et al., 2012). Three-step clustering was performed with raw read filtering and trimming, error-free read selection, and OTU clustering at distant cut-offs (0.03). The taxonomy assignment of bacterial and fungal sequences was based on the full alignments of the 16S rRNA and ITS genes, respectively. Cluster sequences for the 16S rRNA and ITS genes were uploaded to the Silva SSU and UNITE databases, respectively. DNA sequencing was performed by the Macrogen Inc. using the Illumina MiSeq platform according to the

manufacturer's instructions.

Fig. 2.2 Experimental overview of the Illumina MiSeq system of manufacture's intructions (Macrogen Inc.).

Chapter 3
Diversity Estimates of Microbial Communities

3.1 Introduction

Biodiversity is a major theme in ecological research and environmental policy, because diversity may control important ecosystem services (Schimel, 1995). Structural and functional diversity of soil microbes is sensitive to environmental variation, which suggest a wide range of terrestrial ecosystem processes (Schimel, 1995; Balser et al., 2002). Plant species, as a biotic factor are assumed to influence the diversity of microbial communities in the rhizosphere (Berg and Smalla, 2009). Meanwhile, soil microbes contribute to the maintenance of plant species diversity in terrestrial ecosystems (Van Der Heijden et al., 2008). Both soil properties and plant species have effect on the structure and function of microbial communities. However, which factor mainly contributes to microbial communities is difficult to confirm. To investigate soil microbial diversity provides a reasonable way to identify which is the main factor for soil properties changes.

Both microbial species richness and microbial species abundance are taken into account in microbial species diversity. Species richness is the number of different species represented in an ecological community, landscape or region (Colwell, 2009). It is a unit of the number of different microbial species present in an environment. However, microbial species diversity depends not only species on richness, but also on species abundance. Species abundance is the number of individuals per species within a community (Hubbell, 2001). The Shannon and Simpson indices are popular diversity indices in ecological studies. The Shannon

index measures the average degree of uncertainty in predicting which species an individual belongs to at random (Rapidel, 2011). The value of Shannon index increases as the number of species diversity increases. It will be zero if the sample has only one species, and will be maximal when all species in the sample have even abundances (Pylro et al., 2014). Simpson index is more weighted on dominant species compared to Shannon index. The Simpson index reflects species dominance and the probability of individuals that belong to the same species at random. The Simpson index varies from 0 to 1, where the minimum value (0) represents no diversity and the maximum value (1) represents the maximum diversity (Simpson, 1949).

In ecological studies, molecular approaches, especially ribosomal rRNA gene analysis methods, allow complete determinations of the microbial species diversity in a relatively short time without culturing. The phylogenetic identification of microbial species usually relies upon analyses of the highly conserved 16S rRNA gene of bacteria, while both the ITS region and 18S rRNA genes are applied broadly for molecular fingerprinting studies of fungi. However, in fungal communities, the selection of the best phylogenetic gene to use in different molecular methods is still debated. Both the DGGE and NGS techniques have been proven to be very useful for ascertaining the microbial communities of environmental samples. They follow essentially the same initial methodology by targeting and amplifying target genes (Hanning and Ricke, 2011). Using both the DGGE and NGS methods allows

comparisons of microbial populations based on phylogenetic genes, which enables differences in microbial populations to be determined for a wide range of microbial communities. Therefore, in this chapter, the DGGE and NGS methods were used to investigate the species diversity of soil microbial communities in the presence and absence of *S. kurilensis* in a *B. ermanii* forest.

3.2 Comparison of diversity estimates

Several DGGE bands were observed for both the 16S rRNA and 18S rRNA gene samples, which were amplified from DNA isolated from the SI and SR soil samples. According to the number of DGGE bands, diversity estimates were calculated using Quantity One software (Bio-Rad). Quantitative insights into microbial ecology (QIIME) is an open-source bioinformatics pipeline for analyzing microbial diversity from raw DNA sequencing data. It is designed to take users from raw sequencing data generated on the Illumina or other platforms through publication-quality graphics and statistics (http://qiime.org/). In the NGS method, diversity estimates were obtained from DNA sequencing by QIIME software version 1.9.1, which was used to perform alpha-diversity analyses (Chao1, Shannon index, Simpson index) of the bacterial and fungal communities (Caporaso et al., 2010). The Shannon index (H) and Simpson index (λ) account for the relative abundances of all phenotypes. H was calculated using the function $H=-\sum P_i \ln P_i$; λ was calculated using the function $\lambda=1-\sum (P_i)^2$, where *pi* is often the proportion of

individuals belonging to the *i*th species in the given community. To compare the Shannon and Simpson indices between SI plot and SR plot by DGGE and NGS methods, using a one-way analysis of variance (ANOVA) was used to identify significant differences.

3.3 Results

The products of PCR amplification were subjected to DGGE. Dominant band patterns obtained for bacterial communities (Fig. 3.1A) were similar between the SI and SR plots by dominant bands. In contrast to bacterial communities, band patterns obtained for fungal communities (Fig. 3.1B) were observed to show clear difference between the SI and SR plots. The specific bands of fungal communities were indicated in the both SI and SR plots. Two predominant bands were observed in the SI plot, while one was observed in the SR plot (indicated with arrows in Fig. 3.1B). NGS and DGGE methods were used to demonstrate the different values of species richness and diversity estimates. The species richness calculated by the number of bands of DGGE method was lower than that by NGS method (Table 3.1). Both the Shannon and Simpson indices of bacterial and fungal communities were not significantly different in the both SI and SR plots (Fig. 3.2; Fig 3.3).

Table 3.1 Species richness of the bacterial and fungal communities in the SI and SR plots for the five sampling dates by the DGGE and NGS methods.

		DGGE		NGS	
	Dates	SI plot	SR plot	SI plot	SR plot
Bacteria	23 Jul 2014	14	21	847	852
	1 Oct 2014	20	21	960	863
	3 Jun 2015	19	19	935	955
	4 Aug 2015	17	17	919	962
	1 Oct 2015	18	15	1043	998
Fungi	23 Jul 2014	11	16	42	40
	1 Oct 2014	13	21	47	36
	3 Jun 2015	19	22	43	46
	4Aug 2015	20	21	50	46
	1 Oct 2015	19	24	46	44

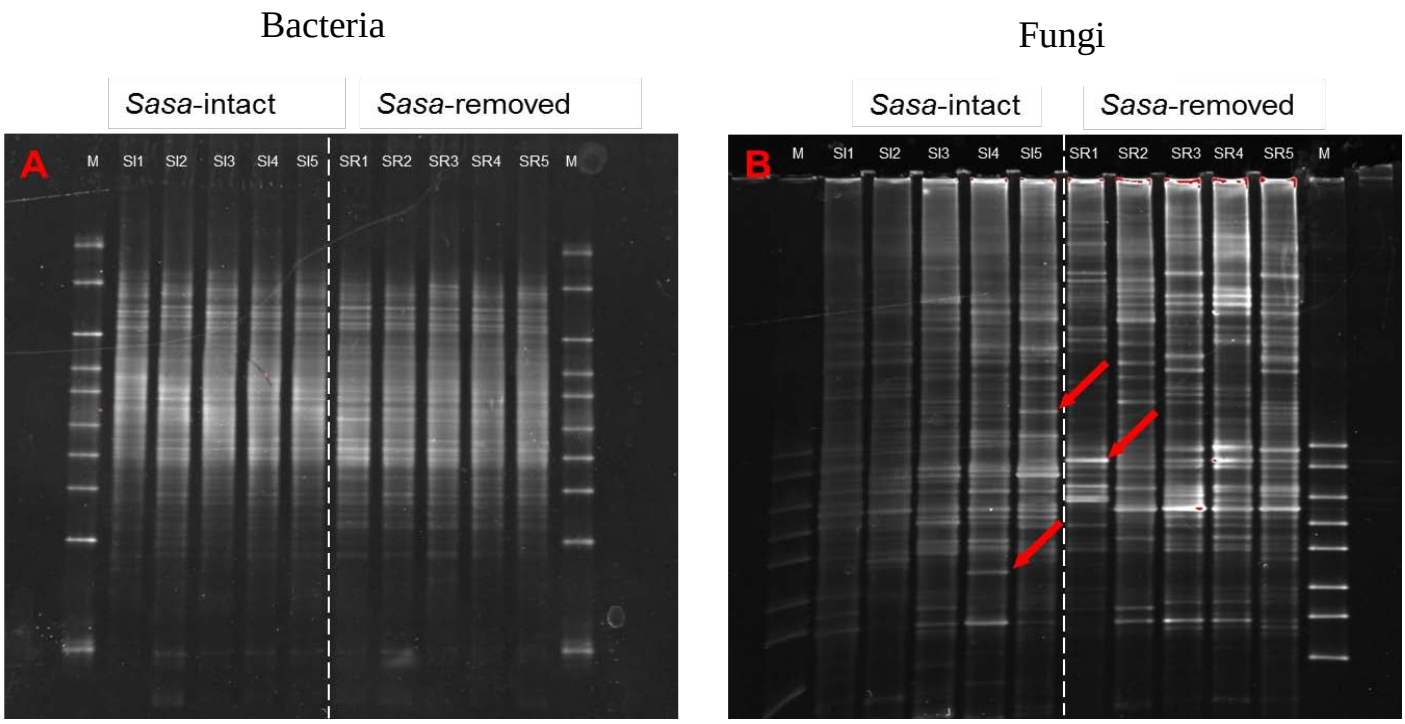

Fig. 3.1 DGGE band profiles of (A) the 16S rRNA gene for bacteria amplicons and (B) the 18S rRNA gene for fungi amplicons in the SI and SR plots. Lanes 1–5 indicate the soil sampling dates of 23 July 2014, 1 October 2014, 3 June 2015, 4 August 2015, and 1 October 2015, respectively. The arrows indicate specific banding patterns. The markers (M) for the 16S and 18S rRNA genes were DGGE Marker III and DGGE Marker IV, respectively.

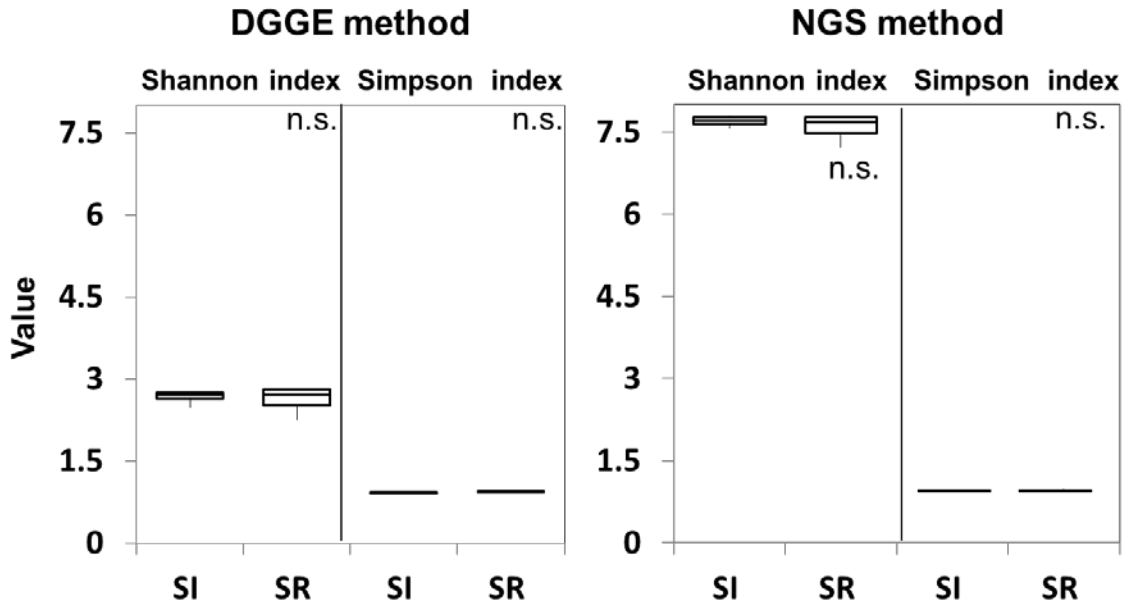

Fig. 3.2 The values of diversity indices of the bacterial communities in the SI and SR plots for the five sampling dates by the DGGE and NGS methods (n.s.: non-significant; one-way ANOVA). Values represent the mean (standard deviation) (n = 5).

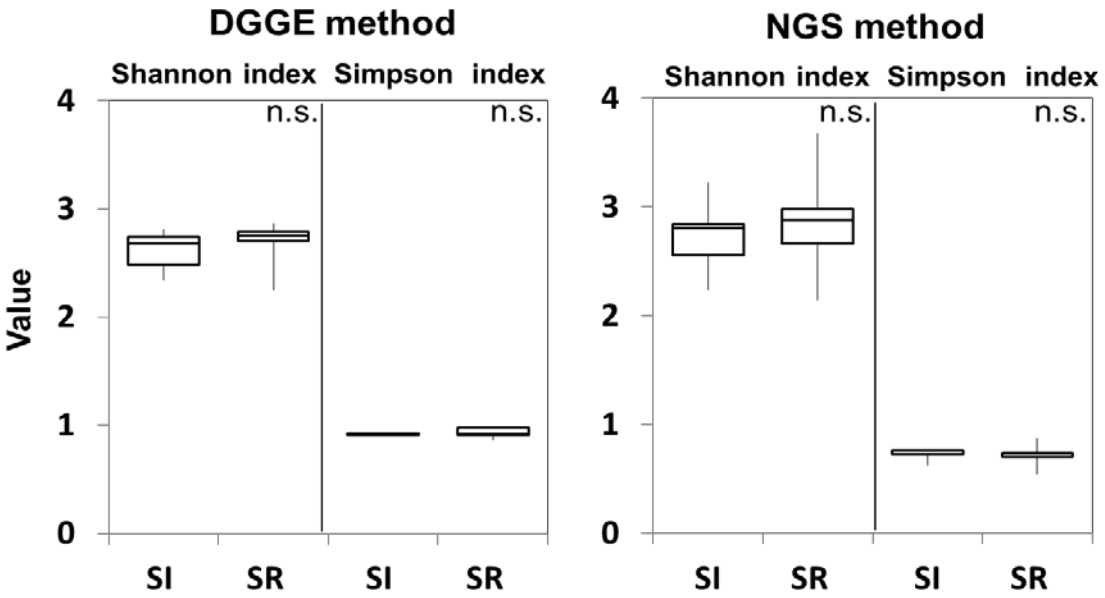

Fig. 3.3 The values of diversity indices of the fungal communities in the SI and SR plots for the five sampling dates by the DGGE and NGS methods methods (n.s.: non-significant; one-way ANOVA). Values represent the mean (standard deviation) (n = 5).

3.4 Discussion

In the Fig. 3.1, both of the bacterial and fungal DGGE patterns obtained from each sample revealed a large number of bands. These results showed the high species diversity of the microbial community in each sample. Comparing the samples between the SI and SR plots, three bands were specific to the fungal communities, while there were few differences in bacterial communities. The shifts of the fungal community structure were affected by the *Sasa*-removal. Thus, these results indicate that *S. kurilensis* affects the fungal community more than the bacterial community in rhizosphere soil.

In the results of species richness, the numbers of OTUs of representatives calculated by DGGE method were lower than by NGS analysis. These results suggested that DGGE analysis might underestimate the species richness of microbial species in soil samples. The Shannon index emphasized the richness component, while the Simpson index emphasized the evenness. In particular, Simpson index is more responsive to dominant cover type to use for single-species reserve design (Nagendra, 2002). In this current study, both the indices of the bacteria and fungi indicated that there were no differences between the SI and SR plots by using the same method (Fig.3.2; Table 3.2). This suggested that the species richness of the bacterial and fungal communities was similar between the two plots whether using DGGE or NGS method. However, DGGE and NGS methods described levels of taxonomic classification from domain to species differently. Díez

et al. (2001) suggested that the DGGE method provides a reasonably detailed, albeit tentative, phylogenetic identification of the dominant community members. Nevertheless, more DNA sequencing information of microbial community structure was necessary to prove the differences between the SI and SR plots. Therefore, I subsequently performed experiments to characterize the differences in the microbial communities between the SI and SR plots using the NGS method.

Chapter 4
Microbial Community Structure and Soil Properties

4.1 Introduction

The nutrients transport in rhizosphere soil is characterized by greater microbiological activity than soil that is located away from plant roots (Osman, 2013). The rhizosphere soil is indispensable for microorganism-driven C sequestration and nutrient cycling in terrestrial ecosystems (Berg and Smalla, 2009). Previous studies showed that shifts in the structures of bacterial and fungal communities are closely linked to the variability of soil properties (Blagodatskaya and Anderson, 1998; Fierer and Jackson, 2006). The development of mycorrhizal symbiosis increases the ability of roots to absorb nutrients and water from the soil environment (Faber et al., 1991; Marschner and Dell, 1994). Mycorrhizal fungi feed on the uptake of organic C from living plants (Bonfante and Genre, 2010). Consequently, the degree of absorption of C may depend on the unique functional attributes of the rhizosphere microbial communities involved.

In the study plots, the intertwining roots of *S. kurilensis* form rhizomes underground, microbial community structure may influence soil properties of the *S. kurilensis*' s rhizosphere soil. Therefore, it is necessary to investigate the microbial community in the rhizosphere soil of *S. kurilensis* to clarify the relationship between understory plants and soil properties in boreal forests. In this chapter, I used the Illumina MiSeq system to analyze the microbial community structures, with or without *S. kurilensis* in the understory, in a *B. ermanii* stand, and I aimed to determine the relationships between the community structures and the soil

physicochemical properties.

4.2 Statistical analyses

Significant differences in soil physicochemical properties between the SI and SR plots on the five sampling dates were tested using generalized linear mixed models, followed by Tukey's honestly significant difference test. Generalized linear mixed models were also used to examine the relationships between the number of OTUs of the microbial communities and the soil physicochemical properties in the SI and SR plots. Differences between the relative abundances of the microbial communities were tested with the Kruskal–Wallis method (Kruskal and Wallis, 1952). All statistical calculations were conducted in R version 3.2 (R Core Team, 2015). p values <0.05 were considered statistically significant. A redundancy analysis (RDA) is a constrained ordination technique that can be used to test whether the occurrence of microbial communities matches specific environmental source profiles (McKinley et al., 2005; Cookson et al., 2006), and it was performed with abundance and environmental data using Canoco version 4.5 (Ter Braak and Smilauer, 2002).

4.3 Results

4.3.1 Soil characteristics

Significant differences were found between the SI and SR plots for most of

the tested physicochemical soil properties. The soil moisture of the SI plot was clearly lower than that of the SR plot (Fig. 4.1A). Although there was no clear difference in soil temperatures (Fig. 4.1B) and pH (Fig. 4.4), all other values differed significantly between the two plots (Fig. 4.2-4.4). The total C content and C:N ratio were higher in the SI plot than in the SR plot, while the ammonium content was lower, regardless of the sampling dates.. For NO_3-N concentration, it was lower in the SI plot than SR plot all the sampling dates except 23 July 2014. NO_2-N concentration was not detected (<1 mg NO_2-N kg^{-1} soil) during the sampling period (data not shown).

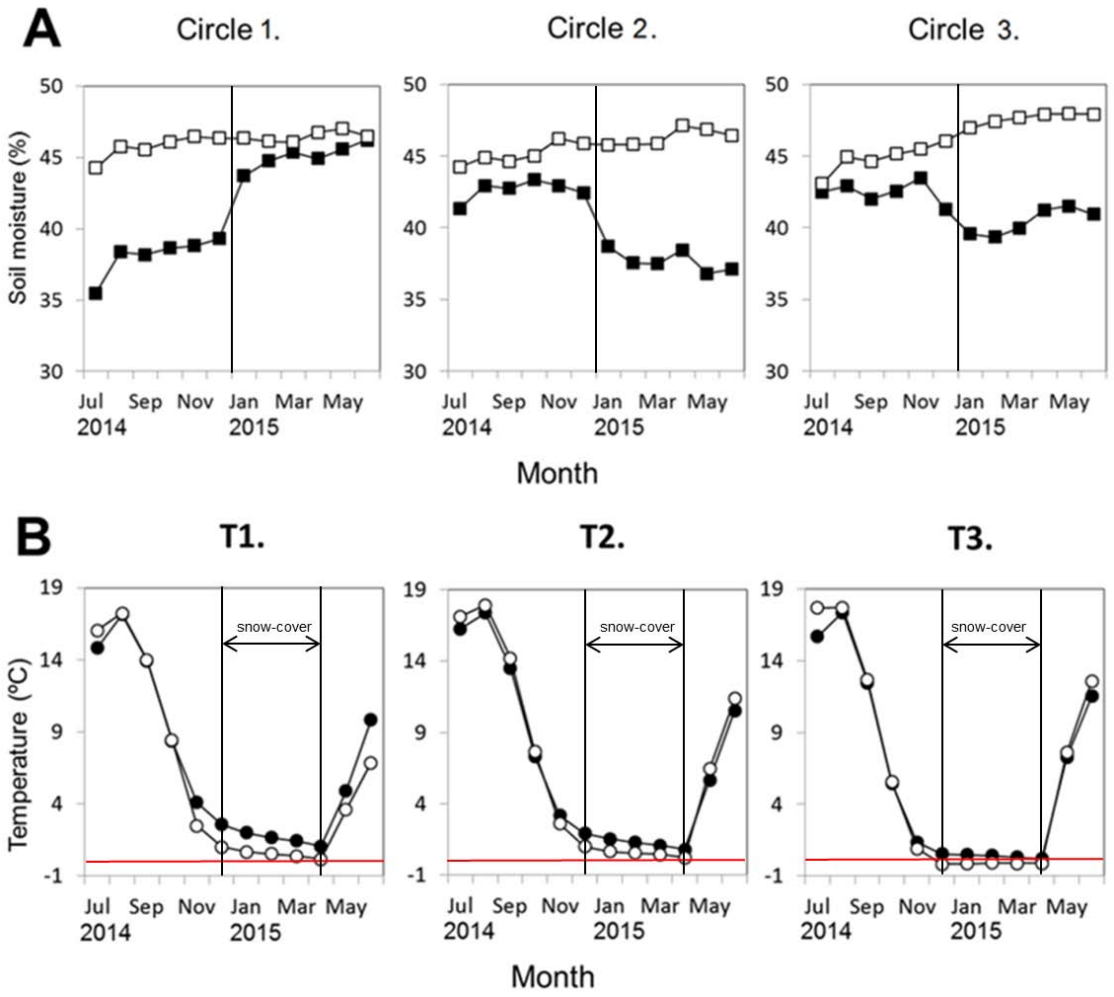

Fig. 4.1. Monthly mean (A) soil moisture (squares) and (B) temperature (circles) of the three sampling circles in the SI (filled) and SR (open) plots between July 2014 and June 2015. T1, air temperature; T2, soil surface temperature; T3, 15-cm-deep soil temperature. Black lines separate soil moisture values of year 2014 and 2015. Red lines represent temperature of 0°C.

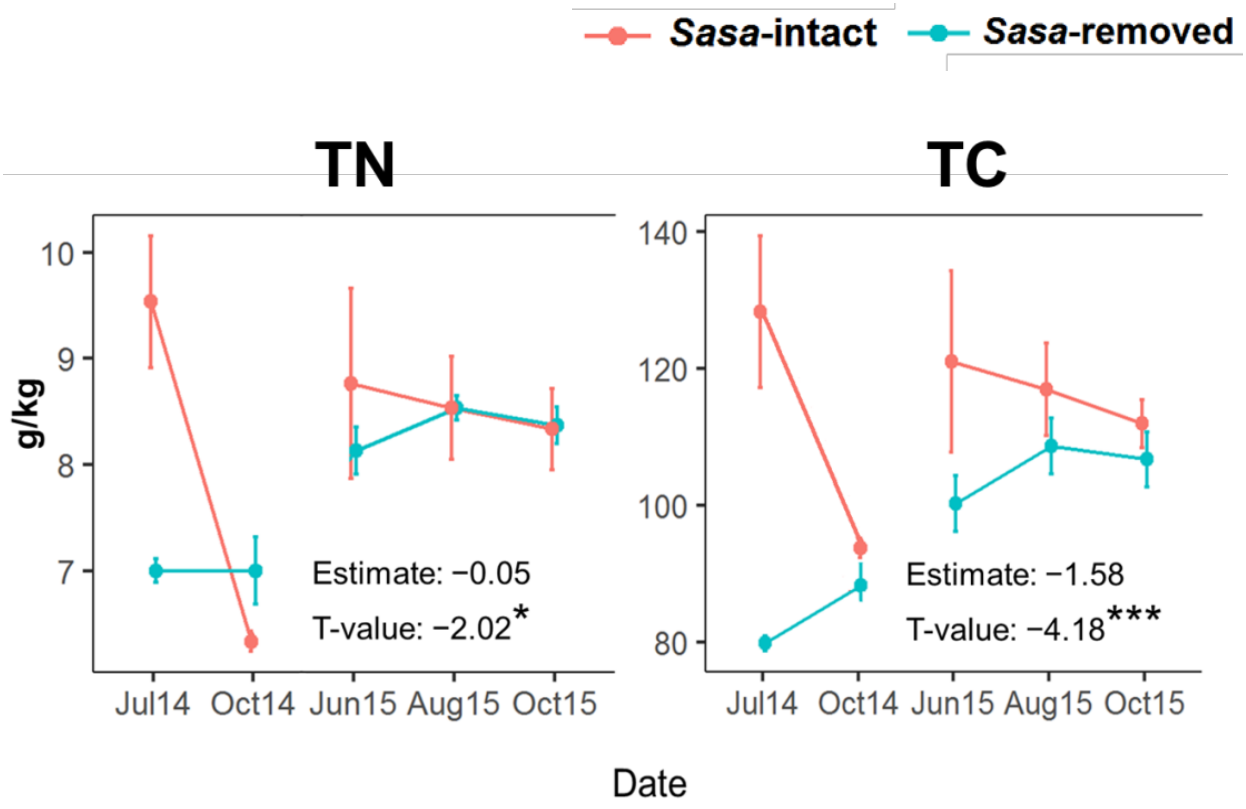

Fig. 4.2. Differences in soil total N and total C contents between the SI and SR plots according to a generalized linear mixed model. The response variable is the concentration of the soil nutrients; the fixed effect is the two study plots; and the random effect is the five sampling dates (n=9). Vertical lines indicate standard errors. *p<0.05; **p<0.01; ***p<0.001; n.s.: non-significant.

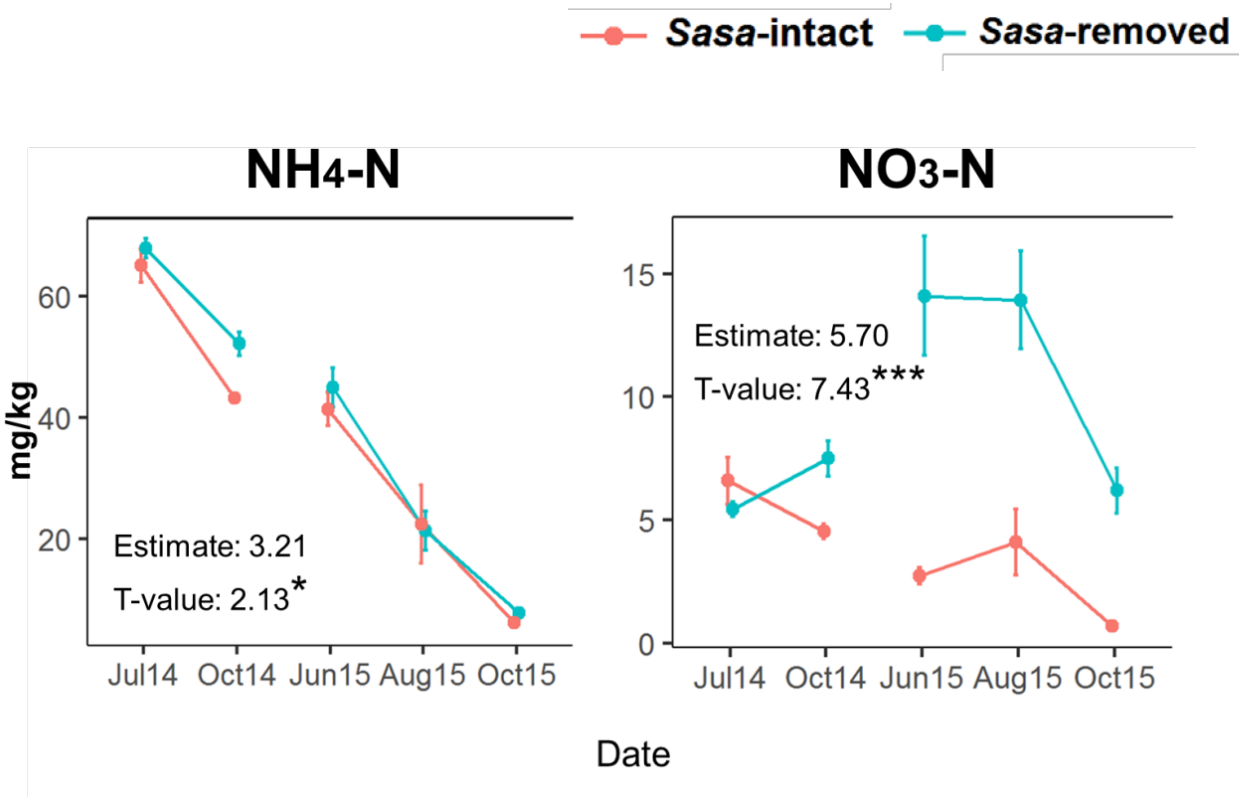

Fig. 4.3. Differences in soil ammonium-N and nitrate-N concentrations between the SI and SR plots according to a generalized linear mixed model. The response variable is the concentration of the soil nutrients; the fixed effect is the two study plots; and the random effect is the five sampling dates (n=9). Vertical lines indicate standard errors. *p<0.05; **p<0.01; ***p<0.001; n.s.: non-significant.

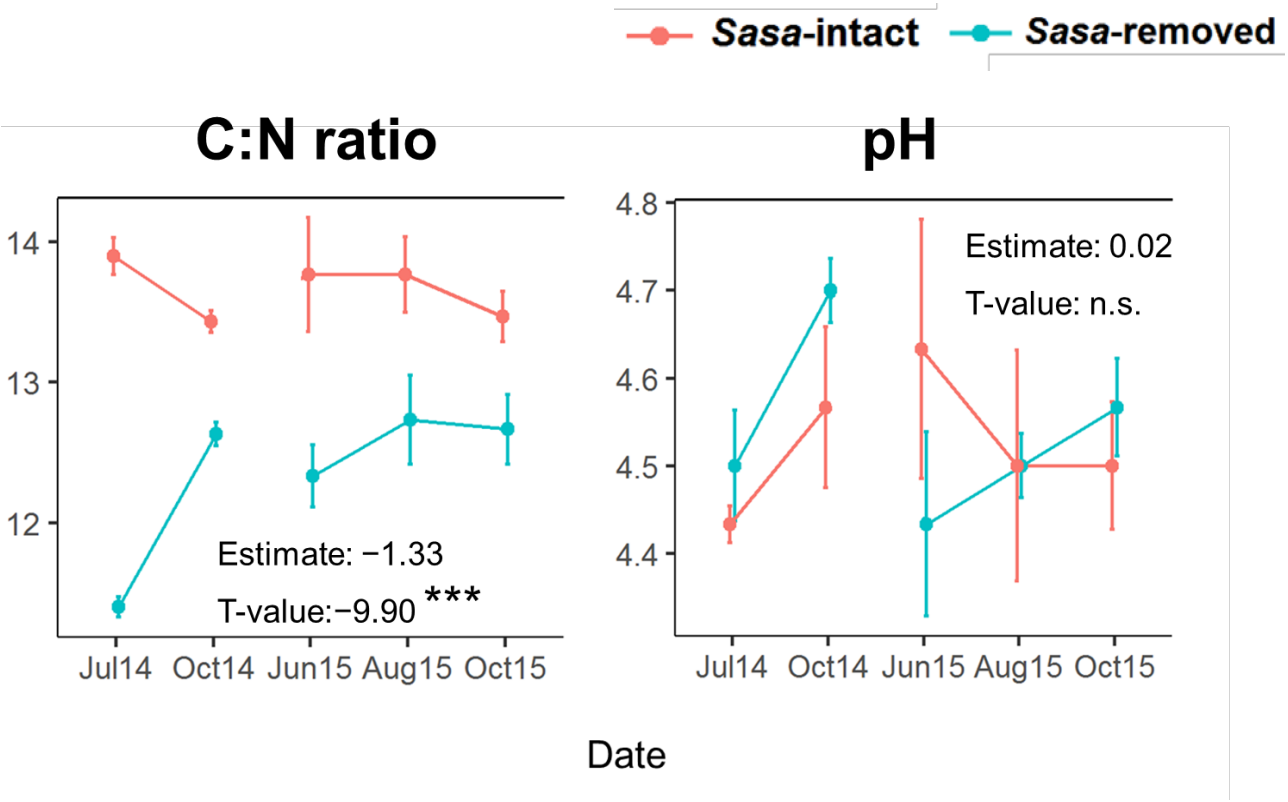

Fig. 4.4. Differences in soil C:N ratio and pH between the SI and SR plots according to a generalized linear mixed model. The response variable is the concentration of the soil nutrients; the fixed effect is the two study plots; and the random effect is the five sampling dates (n=9). Vertical lines indicate standard errors. *p<0.05; **p<0.01; ***p<0.001; n.s.: non-significant.

4.3.2 Abundance of 16S rRNA gene and ITS sequences

After multiple levels of quality control to filter the raw reads, I obtained an average of 26,665 sequences for the 16S rRNA genes for bacteria and an average of 31,080 sequences for the ITS genes for fungi from all the samples. All rarefaction curves were generated via CD-HIT-OTU using a 97% identity cutoff; coverage was greater than 99% for all the samples. These results indicated that the volume of the sequenced reads was reasonable and sufficient to determine the total number of OTUs (Fig. 4.5). Most bacterial samples were saturated at 720–1,125 OTUs, but fungal samples were saturated at 27–55 OTUs. Alpha-diversity of microbial communities was similar in the SI and SR plots. Only the Shannon diversity index for 23 July 2014 was significantly different between the SI and SR plot (Table 4.1).

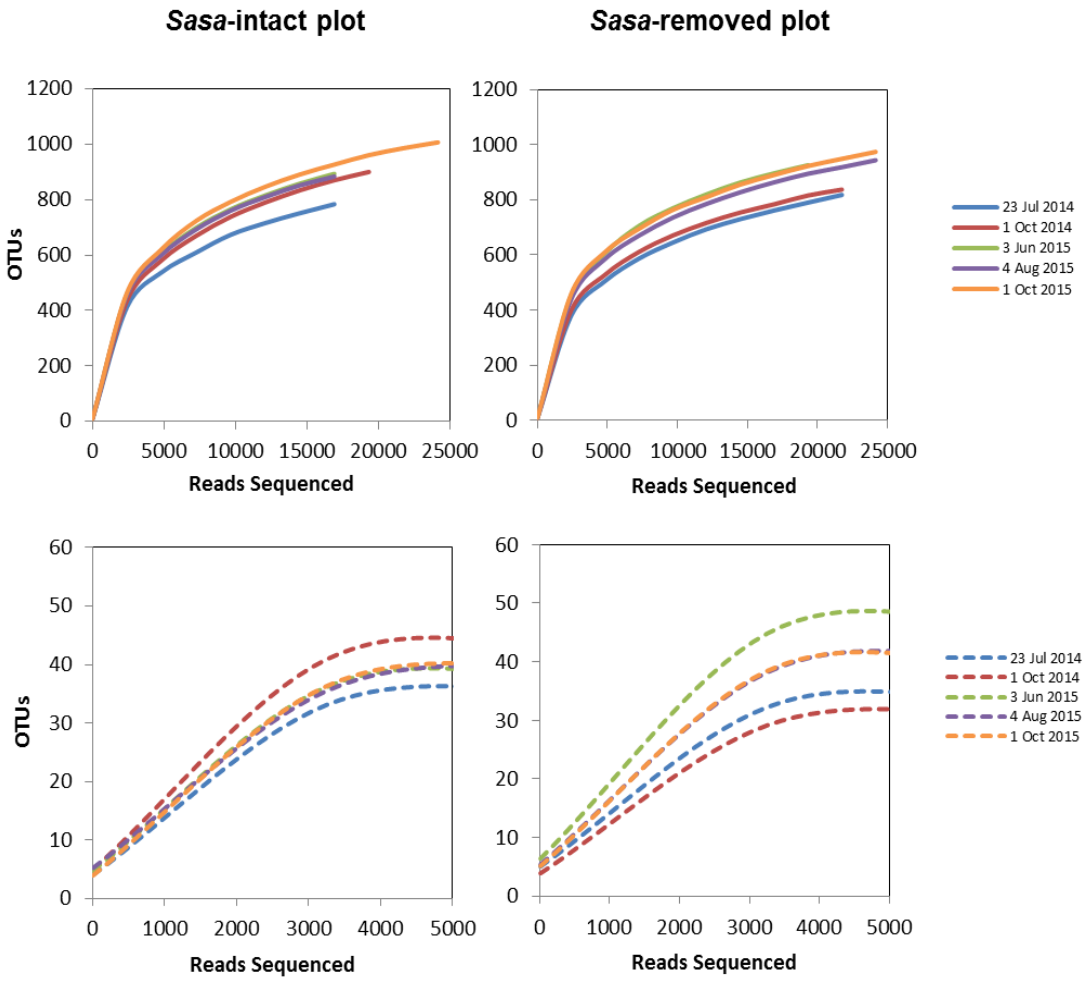

Fig. 4.5. Rarefaction curves for microbial OTUs in the three circles on the five sampling dates, with clustering at a 97% rRNA sequence similarity. Solid and dashed lines represent the OTUs of the bacterial and fungal communities, respectively.

Table 4.1. Alpha-diversity estimates of the microbial communities in the SI and SR plots for the five sampling dates.

		Number of OTUs[a]		Chao1[b]		Shannon[c]		Simpson[d]		Coverage[e]	
	Dates	SI plot	SR plot	SI plot	SR plot	SI plot	SR plot	SI plot	SR plot	SI plot	SR plot
Bacteria	23 Jul 2014	847(64)	852(15)	999(52)	1071(44)	**7.6(0.1)**	**7.2(0.1)**	0.99(0)	0.98(0)	0.99(0)	0.99(0)
	1 Oct 2014	960(37)	863(55)	1141(42)	1021(49)	7.6(0.1)	7.5(0.2)	0.99(0)	0.99(0)	0.99(0)	0.99(0)
	3 Jun 2015	935(31)	955(33)	1146(37)	1138(42)	7.8(0)	7.8(0.1)	0.99(0)	0.99(0)	0.99(0)	0.99(0)
	4 Aug 2015	919(68)	962(48)	1107(90)	1155(49)	7.7(0.2)	7.7(0.1)	0.99(0)	0.99(0)	0.99(0)	0.99(0)
	1 Oct 2015	1043(43)	998(22)	1207(45)	1201(45)	7.8(0.1)	7.8(0.1)	0.99(0)	0.99(0)	0.99(0)	0.99(0)
Fungi	23 Jul 2014	42(1)	40(7)	43(2)	42(7)	2.6(0.4)	2.7(0.2)	0.72(0.06)	0.74(0.02)	1(0)	1(0)
	1 Oct 2014	47(2)	36(4)	50(2)	43(6)	3.2(0.1)	2.1(0.7)	0.77(0.04)	0.55(0.14)	1(0)	1(0)
	3 Jun 2015	43(5)	46(5)	44(6)	48(6)	2.8(0.4)	3.7(0.3)	0.76(0.07)	0.87(0.03)	1(0)	1(0)
	4Aug 2015	50(5)	46(4)	53(5)	46(5)	2.8(03)	2.9(0.7)	0.76(0.06)	0.70(0.16)	1(0)	1(0)
	1 Oct 2015	46(2)	44(4)	46(2)	44(5)	2.2(0.1)	3.0(0.5)	0.62(0.01)	0.73(0.13)	1(0)	1(0)

Note: Values represent the mean (standard deviation) (n = 3). Values in bold denote a significant difference between the SI and SR plots ($p < 0.05$; one-way ANOVA); otherwise, there was no significant difference. [a] Species level, a 97 % similarity threshold was used to define operational taxonomic units (OTUs). [b] Chao1, Chao1 estimator with species richness. [c] Shannon, Shannon Index. [d] Simpson, Simpson Index. [e] Coverage, coverage C was calculated as C=1−(s/n), where s is the number of unique OTUs and n is the number of total reads in the sample.

The bacterial OTUs were assigned to 13 different phyla. Seven different phyla (*Acidobacteria*, *Proteobacteria*, *Bacteroidetes*, *Verrucomicrobia*, *Firmicutes*, *Planctomycetes*, and *Actinobacteria*) comprised more than 90% of the relative abundance in every library (Fig. 4.6A). Because each of the other six phyla comprised <1% of the abundance in both the SI and SR plots, they were excluded from further analyses. Differences between the two plot of the abundance of *Proteobacteria* (20.3% abundance in the SI plot and 17.9% abundance in the SR plot), *Planctomycetes* (4.99% and 5.71%), and *Actinobacteria* (3.43% and 4.01%) were tested by the nonparametric Kruskal–Wallis method, which indicated that there were significant differences between the two plots. The abundances of the other phyla did not differ significantly between the plots: *Acidobacteria* (28.0% abundance in the SI plot and 29.0% abundance in the SR plot), *Bacteroidetes* (18.4% and 17.7%), *Verrucomicrobia* (10.8% and 11.2%), and *Firmicutes* (7.11% and 7.09%). The seven dominant phyla occurred in soil, irrespective of whether *S. kurilensis* was present.

Among phyla *Proteobacteria*, *Planctomycetes* and *Actinobacteria*, abundances of some genera changed after *Sasa*-removal (Fig. 4.7). More specifically, abundance in genera of *Massila* (0.02% abundance in the SI plot and 0.49% abundance in the SR plot), *Acidibacter* (1.86% and 1.11%) and *Rhizomicrobium* (1.25% and 0.87%), belonging to phylum *Proteobacteria*, were significantly different between the SI and SR plots (Fig. 4.7C). Genus of *Sporichthya* (0.02% and 0%) belonging to phylum *Actinobacteria* was not found in the SR plot (Fig 4.7E).

There was no significant difference in *Planctomycetes* genera between the SI and SR plot (Fig. 4.7D).

The numbers of OTUs of the fungal communities was less than those of the bacterial communities. The fungal sequences belonged to four different phyla: *Ascomycota*, *Basidiomycota*, *Zygomycota*, and *Chytridiomycota* (Fig. 4.6B). *Basidiomycota* had average abundances of 64.9% in the SI plot and 67.8% in the SR plot over all the sampling dates. *Zygomycota* had abundances of 15.0% and 17.2% in the SI and SR plots, respectively. *Chytridiomycota* was excluded from further analyses because its abundance was <1% in both plots. Notably, *Ascomycota* had a very different abundance between the two plots, making up 13.9% of the SI plot, but only 0.54% of the SR plot. It showed that the abundance of *Ascomycota* increased with *S. kurilensis*. The relative abundance of the fungal class *Pezizomycetes* (phylum *Ascomycota*) in the SI plot was greater than that in the SR plot (Fig. 4.7F), but *Tremellomycetes* (phylum *Basidiomycota*) was less abundant in the SI plot than in the SR plot for all the sampling dates. Differences in the abundances of the phyla *Ascomycota* and *Basidiomycota* were attributed to the family *Pezizaceae* and the genus *Cryptococcus* (family *Filobasidiaceae*), respectively (Table 4.2). Moreover, the abundance of family of *Sebacinaceae* was 8.69%, only found in the SI plot (Fig. 4.8G).

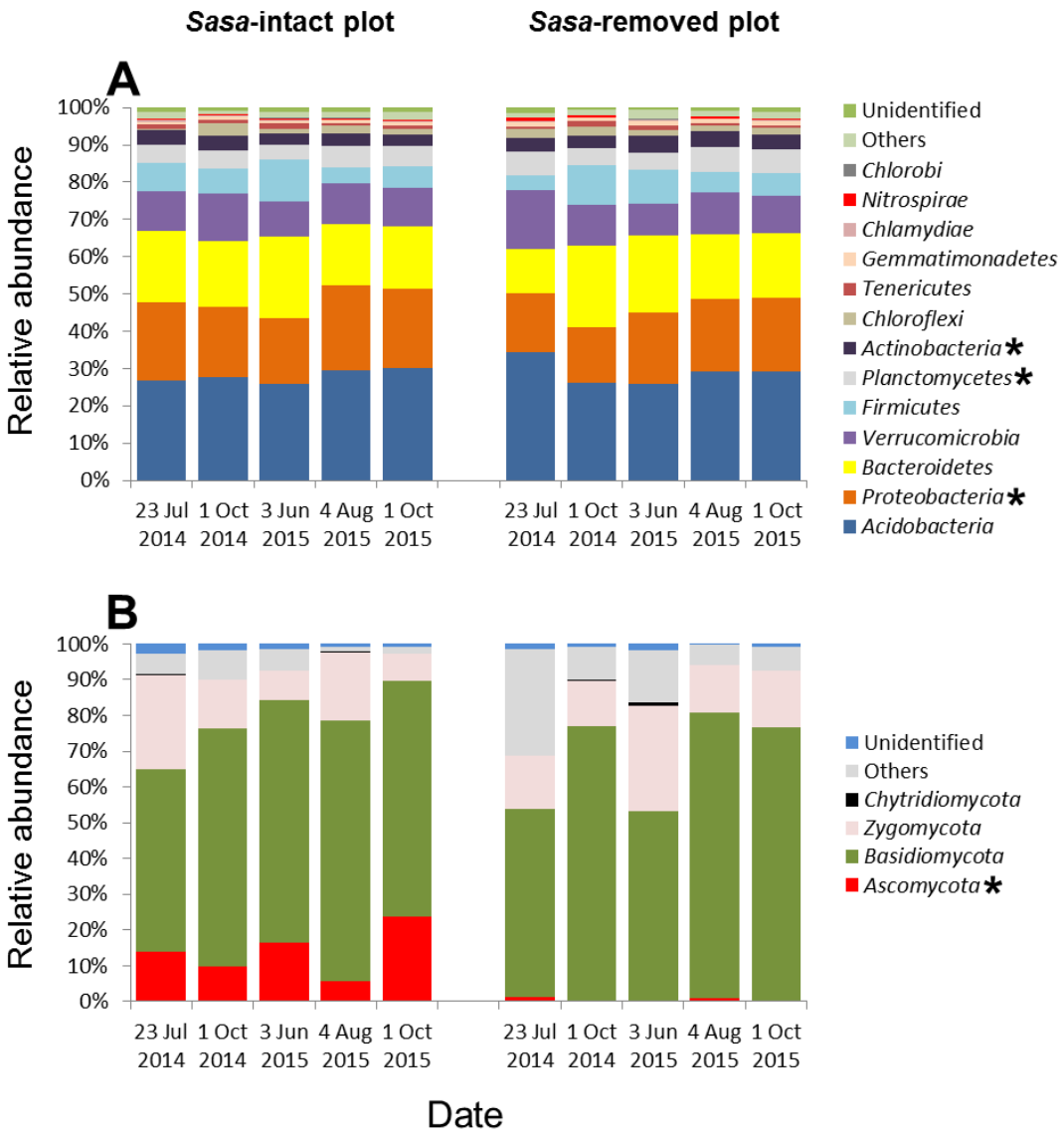

Fig. 4.6. Differences in the relative abundance of the soil microbial communities in *Sasa*-intact and *Sasa*-removed plots for the five sampling dates according to a Kruskal–Wallis test. The asterisk indicates a significant difference (p<0.05; n=15). (A) Bacterial phyla; (B) Fungal phyla.

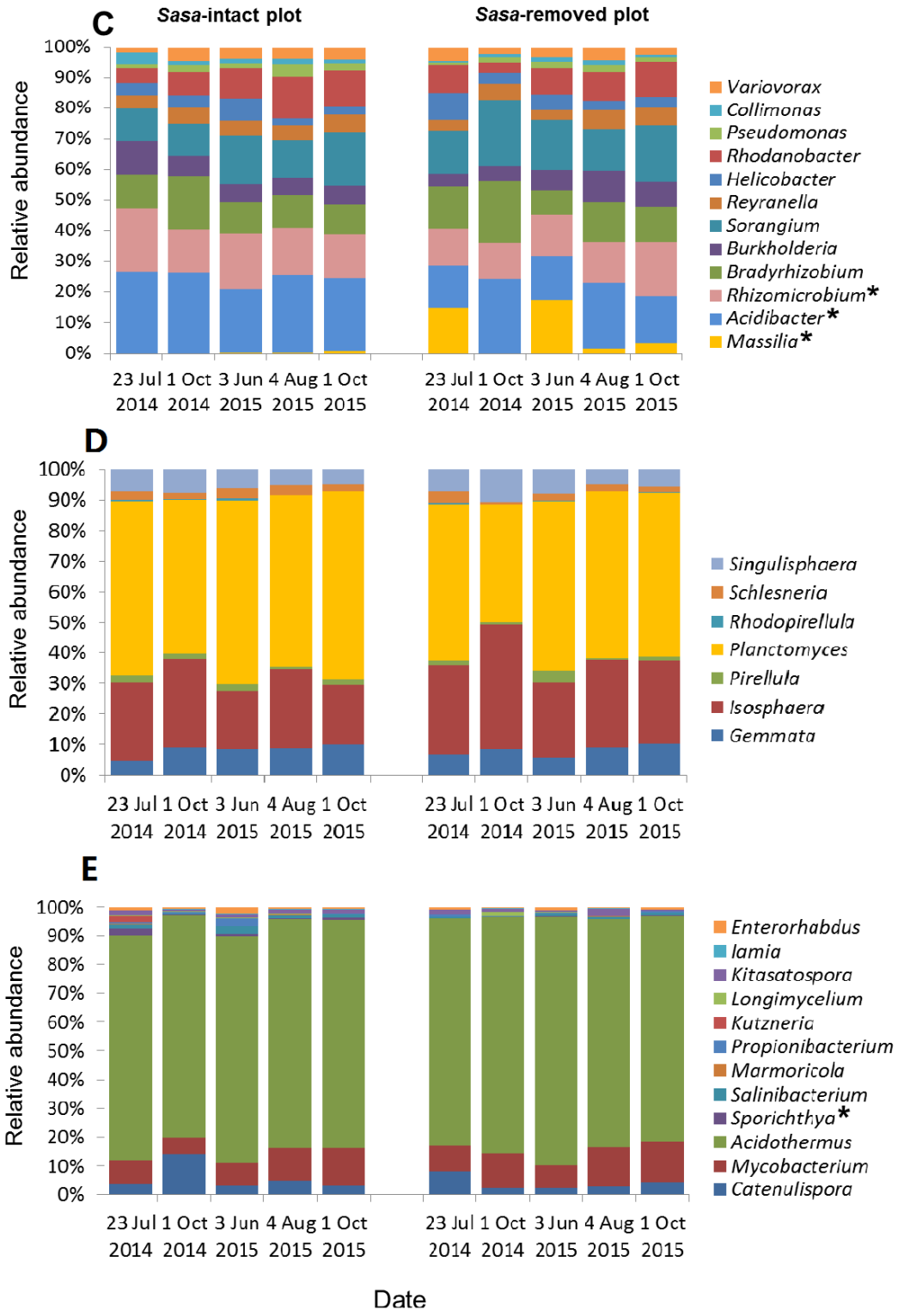

Fig. 4.7. Differences in the relative abundance of the soil microbial communities in *Sasa*-intact and *Sasa*-removed plots for the five sampling dates according to a Kruskal–Wallis test. The asterisk indicates a significant difference (p<0.05; n=15). (C) Genera of *Proteobacteria*; (D) Genera of *Planctomycetes* ; (E) Genera of *Actinobacteria*

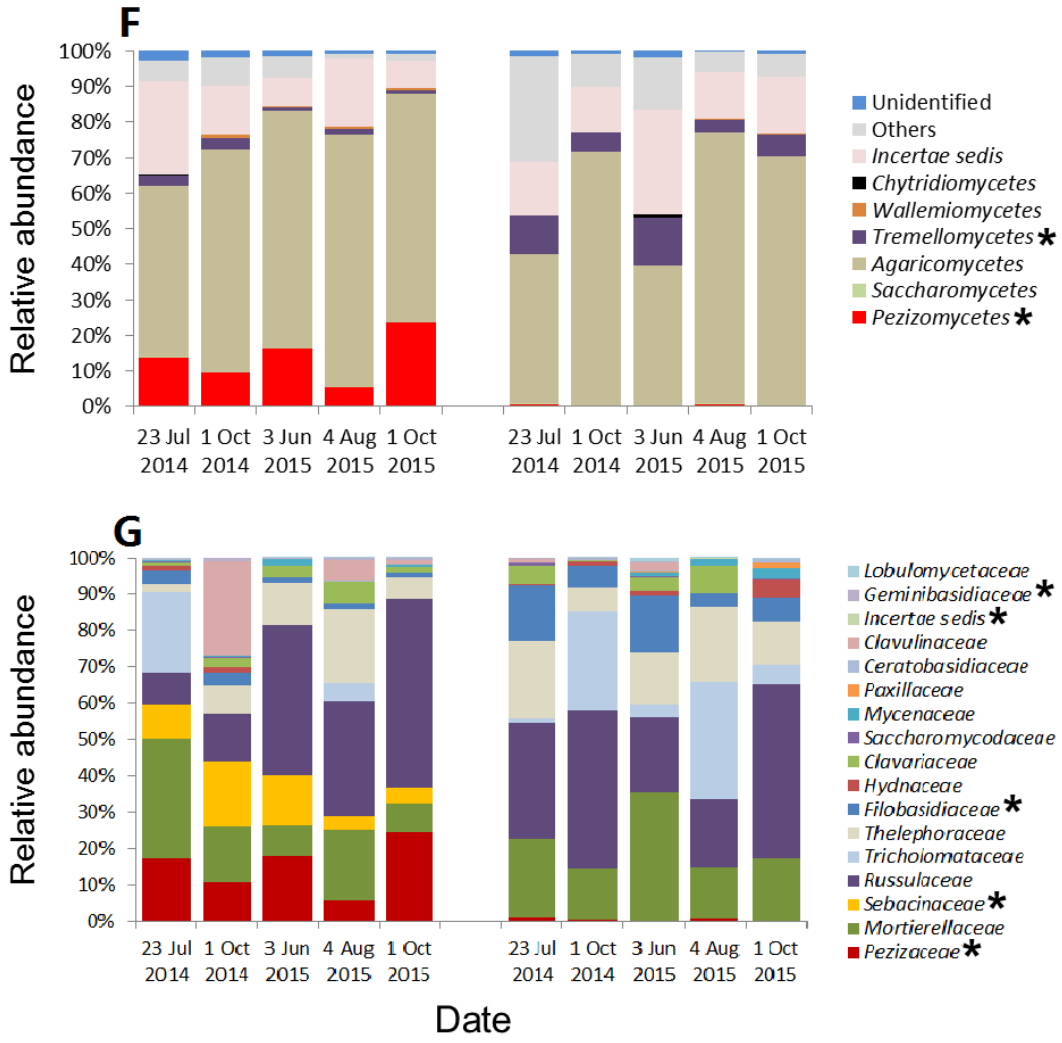

Fig. 4.8. Differences in the relative abundance of the soil microbial communities in *Sasa*-intact and *Sasa*-removed plots for the five sampling dates according to a Kruskal–Wallis test. The asterisk indicates a significant difference (p<0.05; n=15). (A) Fungal classes; (B) Fungal families.

Table 4.2. Percentage (%) of sequences classified for two fungal classes, *Pezizomycetes* and *Tremellomycetes*, in the SI and SR plots for the five sampling dates.

		SI plot					SR plot				
		23 Jul	1 Oct	3 Jun	4 Aug	1 Oct	23 Jul	1 Oct	3 Jun	4 Aug	1 Oct
Dates		2014	2014	2015	2015	2015	2014	2014	2015	2015	2015
Phylum	*Ascomycota*										
Class	*Pezizomycetes*										
Order	*Pezizales*	100	100	100	100	100	100	100	100	100	100
Family	*Pezizaceae*	100	100	100	100	100	100	100	100	100	100
Phylum	*Basidiomycota*										
Class	*Tremellomycetes*										
Order	*Filobasidiales*	100	100	100	98	100	99	100	99	98	99
	Tremellales	0	0	0	2	0	1	0	1	2	1
Family	*Filobasidiaceae*	100	100	100	98	100	99	100	99	98	99
	Incertae sedis	0	0	0	2	0	1	0	1	2	1
Genus	*Cryptococcus*	100	100	100	98	100	99	100	99	98	99
	Unknown spec.	0	0	0	2	0	1	0	1	2	1

4.3.3 Relationships between microbial communities and soil properties

A generalized linear mixed model was used to test whether environmental factors correlated with the relative abundances of microbial species. Table 4.3 shows that *Firmicutes* had a close correlation with the NH_4-N concentration and *Planctomycetes* was strongly correlated with both the TC and TN contents in the SI plot. In the SR plot, the bacterial phylum *Firmicutes* correlated with soil pH, while *Proteobacteria* correlated with the TN content, and the fugal phylum *Basidiomycota* correlated with the NH_4-N concentration.

As shown in Fig. 4.9A, the abundance of phyla *Bacteroidetes* and *Firmicutes* correlated with NO_3-N concentration or pH, and the five other bacterial phyla were each strongly negatively correlated with the TN content, the TC content, the NH_4-N concentration, or the C:N ratio in the SI plot. Although the species richness of fungi was lower than that of bacteria, the RDA analysis showed that the fungal phylum *Basidiomycota* closely correlated with pH. Both the abundance of phyla *Ascomycota* and *Zygomycota* were positively correlated with the TN content, the TC content, the NH_4-N concentration, and the C:N ratio in the SI plot, but they were negative correlated with the NO_3-N concentration in the SR plot (Fig. 4.9B).

Table 4.3. Relationship between soil properties and the number of OTUs of the main phyla in the SI and SR plots based on a generalized linear mixed model.

	Phylum	Soil properties	Intercept	Estimate	SE	*z*-value	*p*
SI plot							
	Acidobacteria	Total nitrogen	−2.28	0.17	0.17	0.99	0.32
		Total carbon	−2.28	0.01	0.01	1.05	0.3
		Ammonium	−2.14	0.02	0.03	0.81	0.42
		Nitrate	−2.18	0.01	0.01	1.15	0.25
		C:N ratio	−2.54	0.03	0.05	0.63	0.53
		pH	−1.45	−0.15	0.12	−1.25	0.21
	Actinobacteria	Total nitrogen	−2.95	0.15	0.23	0.64	0.52
		Total carbon	−2.93	0.01	0.02	0.58	0.56
		Ammonium	−2.83	0.06	0.04	1.49	0.14
		Nitrate	−2.89	0.02	0.01	1.28	0.2
		C:N ratio	−3.19	0.03	0.06	0.42	0.68
		pH	−2.16	−0.15	0.16	−0.9	0.37
	Bacteroidetes	Total nitrogen	−1.77	0.03	0.15	0.18	0.86
		Total carbon	−1.77	0	0.01	0.23	0.82
		Ammonium	−1.75	0.02	0.02	0.86	0.39
		Nitrate	−1.73	0	0.01	−0.38	0.71
		C:N ratio	−1.66	−0.01	0.04	−0.16	0.87

	pH	−2.06	0.07	0.1	0.67	0.51
Firmicutes	Total nitrogen	−2.07	−0.13	0.21	−0.62	0.54
	Total carbon	−2.07	−0.01	0.01	−0.66	0.51
	Ammonium	−2.17	0.11	0.03	3.77	**<0.001**
	Nitrate	−2.25	0.02	0.01	1.38	0.17
	C:N ratio	−1.66	0	0.05	0.02	0.99
	pH	−2.1	−0.02	0.13	−0.12	0.9
Planctomycetes	Total nitrogen	−1.47	0.34	0.15	−2.23	**0.03**
	Total carbon	−1.44	0.03	0.01	−2.58	**0.01**
	Ammonium	−1.74	0.05	0.03	−1.83	0.07
	Nitrate	−1.71	0.01	0.01	−0.96	0.34
	C:N ratio	−0.94	0.06	0.04	−1.4	0.16
	pH	−2.26	0.12	0.11	1.08	0.28
Proteobacteria	Total nitrogen	−1.32	−0.03	0.13	−0.2	0.84
	Total carbon	−1.33	0	0.01	−0.05	0.96
	Ammonium	−1.34	−0.03	0.02	−1.33	0.18
	Nitrate	−1.32	−0.01	0.01	−0.67	0.5
	C:N ratio	−1.4	0	0.04	0.13	0.9
	pH	−1.53	0.04	0.09	0.45	0.66
Verrucomicrobia	Total nitrogen	−2.91	0.23	0.22	1.07	0.28

	Total carbon	−2.87	0.01	0.01	0.92	0.36
	Ammonium	−2.72	0.02	0.04	0.65	0.51
	Nitrate	−2.75	0.01	0.01	0.52	0.6
	C:N ratio	−2.38	−0.02	0.06	−0.41	0.68
	pH	−2.56	−0.04	0.16	−0.23	0.82
Ascomycota	Total nitrogen	−3.48	0.34	1.19	0.28	0.78
	Total carbon	−3.38	0.02	0.08	0.19	0.85
	Ammonium	−3.34	0	0.01	0.38	0.71
	Nitrate	−3.33	0.03	0.08	0.43	0.67
	C:N ratio	−2.48	−0.05	0.36	−0.15	0.86
	pH	−1.74	−0.32	1.06	−0.31	0.76
Basidiomycota	Total nitrogen	−0.44	−0.09	0.49	−0.18	0.86
	Total carbon	−0.47	0	0.03	−0.11	0.91
	Ammonium	−0.46	0	0	−0.38	0.7
	Nitrate	−0.46	−0.02	0.03	−0.47	0.64
	C:N ratio	−0.77	0.02	0.15	0.13	0.9
	pH	−2.33	0.4	0.41	0.99	0.32
Zygomycota	Total nitrogen	−1.31	0.08	0.56	0.15	0.88
	Total carbon	−1.35	0.01	0.04	0.25	0.8
	Ammonium	−1.38	0	0	0.85	0.4

		Nitrate	−1.29	0.01	0.04	0.38	0.7
		C:N ratio	−2.58	0.1	0.17	0.58	0.56
		pH	1.21	−0.54	0.49	−1.1	0.27
SR plot							
	Acidobacteria	Total nitrogen	−1.86	−0.34	0.35	−0.99	0.32
		Total carbon	−1.96	−0.02	0.02	−0.84	0.4
		Ammonium	−2.13	0.02	0.03	0.83	0.41
		Nitrate	−2.08	−0.01	0.01	−1.01	0.31
		C:N ratio	−1.93	−0.02	0.04	−0.4	0.69
		pH	−2.03	−0.02	0.16	−0.14	0.89
	Actinobacteria	Total nitrogen	−2.88	0.08	0.47	0.16	0.87
		Total carbon	−2.92	0.01	0.03	0.38	0.71
		Ammonium	−2.82	0	0.04	0.05	0.96
		Nitrate	−2.8	0	0.01	−0.3	0.76
		C:N ratio	−3.25	0.03	0.06	0.63	0.53
		pH	−1.97	−0.19	0.21	−0.9	0.37
	Bacteroidetes	Total nitrogen	−1.87	0.19	0.34	0.58	0.56
		Total carbon	−1.82	0.01	0.02	0.56	0.58
		Ammonium	−1.72	0	0.03	−0.11	0.91
		Nitrate	−1.77	0	0	0.96	0.34
		C:N ratio	−2	0.02	0.04	0.59	0.55

	pH	−1.39	−0.07	0.14	−0.51	0.61
Firmicutes	Total nitrogen	−1.5	−0.82	0.44	−1.87	0.06
	Total carbon	−1.91	−0.02	0.03	−0.91	0.37
	Ammonium	−2.15	0.01	0.06	0.18	0.85
	Nitrate	−2.07	−0.01	0.01	−1.16	0.25
	C:N ratio	−2.82	0.05	0.05	1.07	0.29
	pH	−0.46	−0.37	0.18	−2.09	**0.04**
Planctomycetes	Total nitrogen	−1.45	−0.28	0.36	−0.76	0.45
	Total carbon	−1.49	−0.02	0.02	−0.9	0.37
	Ammonium	−1.67	0	0.03	0.06	0.95
	Nitrate	−1.66	0	0.01	−0.18	0.86
	C:N ratio	1.17	−0.04	0.04	−1.05	0.3
	pH	−2.61	0.21	0.14	1.44	0.15
Proteobacteria	Total nitrogen	−1.84	0.61	0.27	2.27	**0.02**
	Total carbon	−1.63	0.03	0.02	1.77	0.08
	Ammonium	−1.37	−0.04	0.02	−1.64	0.1
	Nitrate	−1.43	0.01	0	1.76	0.08
	C:N ratio	−1.44	0.01	0.03	0.2	0.84
	pH	−1.48	0.02	0.12	0.21	0.84
Verrucomicrobia	Total nitrogen	−3.3	0.7	0.46	1.54	0.12

	Total carbon	−3.06	0.03	0.03	1.18	0.24
	Ammonium	−2.75	−0.02	0.04	−0.63	0.53
	Nitrate	−2.81	0.01	0.01	0.87	0.38
	C:N ratio	−2.81	0	0.05	0.09	0.93
	pH	−3.15	0.09	0.21	0.43	0.67
Ascomycota	Total nitrogen	−3.72	0.54	2.83	0.19	0.85
	Total carbon	−3.65	0.04	0.16	0.22	0.82
	Ammonium	−3.46	0	0.01	0.43	0.67
	Nitrate	−3.33	0	0.04	0.07	0.95
	C:N ratio	−3.75	0.04	0.32	0.11	0.91
	pH	−1.85	−0.32	1.25	−0.26	0.8
Basidiomycota	Total nitrogen	0.66	−1.42	1.06	−1.34	0.18
	Total carbon	0.48	−0.1	0.06	−1.56	0.11
	Ammonium	−0.75	0.01	0	2.08	**0.04**
	Nitrate	−0.43	0	0.02	−0.19	0.85
	C:N ratio	1.95	0.04	0.32	0.11	0.91
	pH	−1.33	0.19	0.49	−0.39	0.7
Zygomycota	Total nitrogen	−0.45	−1.06	1.25	−0.85	0.39
	Total carbon	−0.76	−0.05	0.07	−0.74	0.46
	Ammonium	−1.46	0	0	1.06	0.29

Nitrate	−1.34	0.01	0.02	0.33	0.74
C:N ratio	−0.8	−0.04	0.14	−0.27	0.79
pH	−0.82	−0.1	0.57	−0.18	0.86

Note: The response variable is the number of OTUs of the main phyla. The fixed effect is the value of the soil properties, and the random effect is the two study plots. Significance at the $p<0.05$ level is shown in bold.

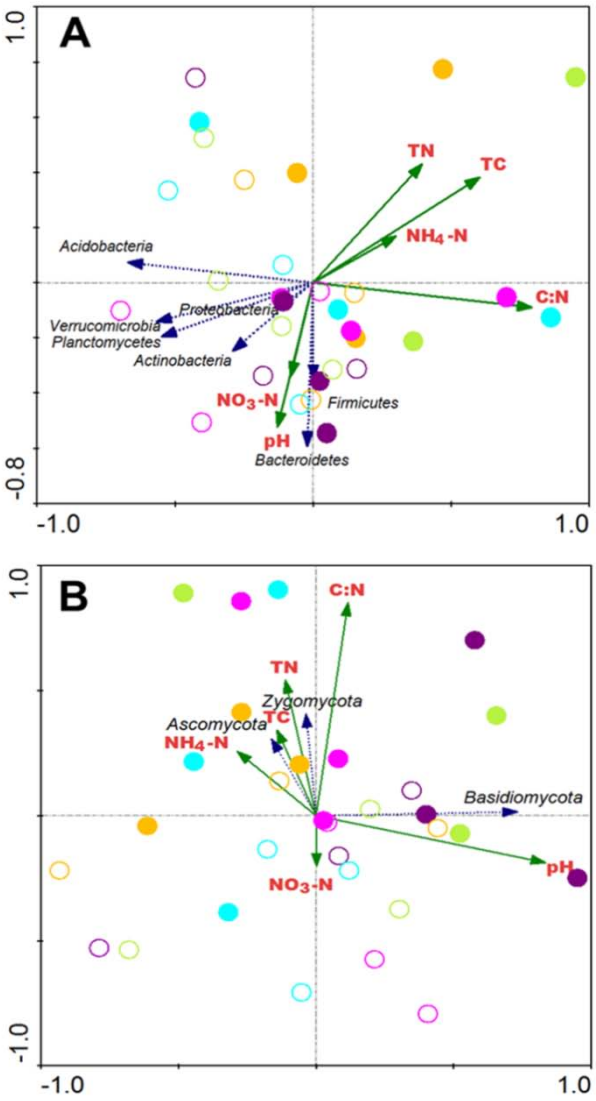

Fig. 4.9. Redundancy analysis of main (A) bacterial and (B) fungal communities in *Sasa*-intact (solid circles) and *Sasa*-removed (open circles) plots based on Canoco 4.5. The purple, light green, orange, aqua, and pink colors represent the sampling dates of 23 July 2014, 1 October 2014, 3 June 2015, 4 August 2015, and 1 October 2015, respectively. Blue and dark green arrows indicate the abundance of microbes and values of soil properties, respectively. TN: total nitrogen; TC: total carbon; NH_4-N: ammonium; NO_3-N: nitrate.

4.4 Discussion

4.4.1 Soil properties before and after the removal of *Sasa kurilensis*

Although the locations of experimental plots were relatively close, there were changes in soil properties after *Sasa kurilensis* (hereafter "*Sasa*") was removed. In this study, SR soil was wetter than SI soil during the whole year (Fig. 4.1A). Moreover, the difference in soil moisture between the maximum and minimum in the SI plot was greater than that in the SR plot. This might be because the growth of *Sasa* would consume a large amount of water through water absorption by root and transpiration from leaves.

In addition, soil C content was higher in the SI plot than in the SR plot. Before this experiment, *Sasa* above the ground had been continuously removed by trimmers and sickles in the SR plot for almost 16 years. Due to the absence of leaves and stems aboveground, the activity of the culm and rhizome of *Sasa* underground would have been decreased and the microbial biomass of rhizosphere soil of *Sasa* could have changed after the removal of *Sasa*. The higher TC contents and C: N ratios in the SI plot in this study (Fig. 4.2; Fig 4.4) suggest that rhizosphere soil of *Sasa* stored more C and that the rhizome of *Sasa* is an important organ to store C in the soil.

4.4.2 Bacterial community structure and soil properties

Microbes play an important role in the function of ecosystems (e.g., biodiversity or stability)(Lladó et al., 2017). In the following discussion, I

comment on potential function(s) of several bacterial and fungal communities identified in this study. Many phyla of bacteria that are widespread in nature have been found in the rhizophere soil. For example, the strains belonging to *Proteobacteria* and *Actinobacteria* have been identified as mycorrhizal helper bacteria (MHB) (Frey et al., 1997; Frey-Klett et al., 2007).

As the second largest bacteria group in the two plots, the abundance of the *Proteobacteria* group was significantly different between the SI and the SR plots. At the genus level (Fig 4.7C), the abundance of genera *Massilia*, *Acidibacter* and *Rhizomicrobium* varied greatly after the removal of *Sasa*. The abundance of *Massilia* was much lower in the SI plot than in the SR plot. In addition, in the SR plot, the abundance of genus *Massilia* was observed to peak on 23 July 2014 and 3 June 2015. Because *Massilia* is known to form copiotrophic and competition-sensitive root colonization (Ofek et al., 2012), the presence of *Sasa* may inhibit the growth of *Massilia*. Genus *Acidibacter* was characterized as a novel genus, and the first found representative species is *Acidibacter ferrireducens*, which can live in extremely acidic environments (Falagán and Johnson, 2014). Genus *Rhizomicrobium* is root-exudate-favored and symbiotic N-fixing bacteria (Nguyen et al., 2016; Ishaq et al., 2017). It suggests that *Sasa* might affect the abundance of genera *Acidibacter* and *Rhizomicrobium* by influencing soil properties.

Phylum *Planctomycetes* is likely to be dominant in wet environments. A previous study found that phylum *Planctomycetes* lived with ectomycorrhizal

fungi, which is related to C cycle in the boreal forest soil (Lindahl et al., 2010). In addition, the number of OTUs of phylum *Planctomycetes* was positively correlated with the amount of soil TC. It suggests that *Sasa* could affect the community structure of phylum *Planctomycetes* through increasing the soil TC.

In general, the abundance of most bacterial communities was greater in the SR plot than in the SI plot (Fig. 4.9A). However, since some significant relationships were detected between the number of OTUs of phyla present and environmental factors, this co-occurrence may be an artefact due to mutual dependence on the same environmental factors. Therefore, it is necessary to conduct a further experiment that analyzes the functions at the species level by using cultural methods.

4.4.3 Fungal community structure and soil properties

In the current study, the abundance of fungal communities (Fig. S2) in the SI plot was higher than in the SR plot. Correspondingly, the TC contents and the C:N ratios (Fig. 4.2; Fig. 4.4) were also higher in the SI plot than in the SR plot. It suggests that the fungal community plays a more important role than the bacterial community in the soil C cycle and storage of boreal forests (Malik et al., 2016).

Order *Pezizales* was important root-associated fungi in the roots of piñon pine and juniper trees in arid woodlands and savannas (Dean et al., 2015). In addition, family *Pezizaceae* is known to act as ectomycorrhizal fungi under

drought conditions (Hansen and Pfister, 2006; Gordon and Gehring, 2011). Similarly, a larger number of mycorrhizal fungi *Pezizaceae* which were predominant among the identified phylum *Ascomycota* were found in the drier SI plot (Fig. 4.8G; Table 4.2). This result suggests that *Pezizaceae* favors living in drier soil conditions. Furthermore, C:N ratio in the SI plot was greater than that in the SR plot. It suggests that family *Pezizaceae* prefers to survive in soil conditions with relatively lower N content. A possible interpretation is that fungal mycelium grows better in soils with lower nitrogen content to absorb more C from plant roots under such conditions (Garcia et al., 2015). Root-associated *Ascomycota* can thrive in stressed environments because their mycelium has a complex structure of fungal cell walls that contain chitin and melanin and are resistant to microbial degradation (Coelho et al., 1997; Butler and Day, 1998). As a result, *Ascomycota* mycelia tend to leave a large amount of fungal necromass that serves to store C in the boreal soil (Clemmensen et al., 2015; Fernandez et al., 2016). The results of Fig. 4.9B show that the abundance of mycorrhizal fungi of phylum *Ascomycota* increased with the increase in TC content in the SI plot; however, *Ascomycota* species richness was low (Fig. 4.5). If the abundance of this mycorrhizal fungus is in parallel with its biomass, one possible explanation for the greater TC in the SI plot is a close relationship between the presence of *Sasa* and the mycorrhizal family *Pezizaceae* (phylum *Ascomycota*), and the existence of this fungal family appeared to increase the TC content in the SI soil. Further studies are needed to confirm this hypothesis.

Phylum *Basidomycota* was the most abundant in both the SI and SR plots. In this phylum, the abundance of family *Filobasidiaceae* (class *Tremellomycetes*) in the SR plot was greater than in the SI plot (Fig. 4.8G). Vishniac (2006) found that genus *Cryptococcus*, which was predominant among the identified family *Filobasidiaceae* (Table 4.2), preferred wet soils to dry soil. Therefore, family *Filobasidiaceae* was more abundant in the SR plot due to its higher soil moisture. Species in family *Sebacinaceae* can form mycorrhizas with a wide variety of plants in boreal mixed forests (Tedersoo et al., 2003). In this study, family *Sebacinaceae* was found only in the SI plot (Fig. 4.8G). It suggests that the roots of *Sasa* can form mycorrhizas with family *Sebacinaceae* in the rhizosphere soil.

In addition, the abundance of fungal families in the SI plot showed greater variation than in the SR plot (Fig. 4.8G). Similar to the main results by DGGE method in Chapter 3, the fungal community structure is more likely to be impacted by the removal of *Sasa* than the bacterial community structure, indicating that *Sasa kurilensis* probably serves as a host species for the mycorrhizal fungi.

Chapter 5

Conclusions and Future Work

In this dissertation, I characterized the microbial community structure in the rhizosphere soil of *S. kurilensis* in a *B. ermanii* boreal forest. This study provided strong evidence showing the close relationship between the microbial community structure and the soil properties in study plots. DGGE was used initially in a preliminary experiment to evaluate the microbial community structure in the environment, while NGS method may be more widely used in the research of microbial taxonomy. By analyzing a DGGE fingerprint gel, I found that *S. kurilensis* affect the community structure of the fungal communities more than that of the bacterial communities. The Shannon and Simpson indices of the bacterial and fungal communities were similar in both the *Sasa*-intact plot and *Sasa*-removed plots, which indicated the same microbial species richness between the two plots based on the DGGE method and NGS method.

This study also indicated that the presence of *S. kurilensis* in a *B. ermanii* boreal forest affected the structures of the soil fungal and bacterial communities and the corresponding soil properties. Moreover, a novel finding is that the presence of *S. kurilensis* likely promoted the colonization of soil mycorrhizal fungi of the family *Pezizaceae* (phylum *Ascomycota*), which may mediate soil carbon. The present study enriches our understanding of how the presence of understory bamboo affects soil properties and the corresponding microbial communities in a boreal forest. Many studies have elucidated the mechanisms underlying carbon sequestration in boreal forests, and they showed the importance of root-associated fungi for ecosystem carbon balances. Thus, the increasing spread

of *S. kurilensis* may support the carbon sink function of boreal forests in northern Japan. Due to the close relationship between mycorrhizal fungi and soil properties involved *S. kurilensis*, a study of identifying the kind of mycorrhizal fungi of *Pezizaceae*, and further investigate the mechanism of *S. kurilensis* and *Pezizaceae* would contribute to the knowledge of the carbon sink function of boreal forests.

Acknowledgements

First of all, I would like to extend my sincere gratitude to my supervisor, Prof. Dr. Toshihiko Hara for providing me with this precious study opportunity as a Ph.D. student in his laboratory. I am deeply grateful that he was very kind to support all of my new research ideas. High tribute shall be paid to my laboratory members, Associate Prof. Akihiro Sumida, Dr. Kiyomi Ono, Dr. Shigeaki Hasegawa, Dr. Azusa Suzuki-Tabata, Mr. Lei Chen, Mr. Zhou Li and Ms. Moe Wakatsuchi for their support and help throughout the course of my study. I am also deeply indebted to Prof. Ryusuke Hatano, Associate Prof. Yasuhiro Kasahara, Dr. Jan Wild, Dr. Jiri Dolezal and Mr. Arata Nagatake for giving fruitful suggestions and constructive comments during my study. A lot of thanks to Prof. Ayumi Tanaka and Prof. Manabu Fukui and their laboratory members for their kind help when I was working in the Institute of Low Temperature Science (ILTS), Hokkaido University. I especially would like to thank Prof. Pingqing Fu, Dr. Fiolenta Marpaung, Dr. Meirong Chen, Dr. Xiaomeng Zhang, Dr. Mengyao Deng, Ms. Meng Liu, Ms. Jie Chen and lots of my Chinese friends who always supported and encouraged me when I felt down and lonely. Finally, I enormously express appreciation to my husband Kazuaki Kuwahata and my parents for their endless love, understanding and support during these years.

This research was funded by the ILTS, Hokkaido University and the Ministry of Education, Culture, Sports, Science and Technology (MEXT), Japan.

References

Averill, C., Turner, B.L., Finzi, A.C., 2014. Mycorrhiza-mediated competition between plants and decomposers drives soil carbon storage. Nature 505, 543-545.

Baldwin, B.G., 1992. Phylogenetic utility of the internal transcribed spacers of nuclear ribosomal DNA in plants: an example from the Compositae. Molecular Phylogenetics and Evolution 1, 3-16.

Balser, T., Kinzig, A., Firestone, M., 2002. The functional consequences of biodiversity. The Functional Consequences of Biodiversity, Princeton University Press, Princeton, 265-293.

Berg, G., Smalla, K., 2009. Plant species and soil type cooperatively shape the structure and function of microbial communities in the rhizosphere. FEMS Microbiology Ecology 68, 1-13.

Blagodatskaya, E.V., Anderson, T.-H., 1998. Interactive effects of pH and substrate quality on the fungal-to-bacterial ratio and qCO_2 of microbial communities in forest soils. Soil Biology and Biochemistry 30, 1269-1274.

Bonfante, P., Genre, A., 2010. Mechanisms underlying beneficial plant–fungus interactions in mycorrhizal symbiosis. Nature Communications 1, 48.

Butler, M., Day, A., 1998. Fungal melanins: a review. Canadian Journal of Microbiology 44, 1115-1136.

Caporaso, J.G., Kuczynski, J., Stombaugh, J., Bittinger, K., Bushman, F.D., Costello, E.K., Fierer, N., Pena, A.G., Goodrich, J.K., Gordon, J.I., 2010. QIIME allows analysis of high-throughput community sequencing data. Nature Methods 7, 335-336.

Caporaso, J.G., Lauber, C.L., Walters, W.A., Berg-Lyons, D., Huntley, J., Fierer, N., Owens, S.M., Betley, J., Fraser, L., Bauer, M., 2012. Ultra-high-throughput microbial community analysis on the Illumina HiSeq and MiSeq platforms. The ISME journal 6, 1621-1624.

Clemmensen, K.E., Bahr, A., Ovaskainen, O., Dahlberg, A., Ekblad, A., Wallander, H., Stenlid, J., Finlay, R., Wardle, D., Lindahl, B., 2013. Roots and associated fungi drive long-term carbon sequestration in boreal forest. Science 339, 1615-1618.

Clemmensen, K.E., Finlay, R.D., Dahlberg, A., Stenlid, J., Wardle, D.A., Lindahl, B.D., 2015. Carbon sequestration is related to mycorrhizal fungal community shifts during long-term succession in boreal forests. New Phytologist 205, 1525-1536.

Coelho, R., Sacramento, D., Linhares, L., 1997. Amino sugars in fungal melanins and soil humic acids. European Journal of Soil Science 48, 425-429.

Colwell, R.K., 2009. Biodiversity: concepts, patterns, and measurement. The Princeton guide to ecology, 257-263.

Cookson, W., Marschner, P., Clark, I., Milton, N., Smirk, M., Murphy, D., Osman, M., Stockdale, E., Hirsch, P., 2006. The influence of season, agricultural management, and

soil properties on gross nitrogen transformations and bacterial community structure. Soil Research 44, 453-465.

Dean, S.L., Warnock, D.D., Litvak, M.E., Porras-Alfaro, A., Sinsabaugh, R., 2015. Root-associated fungal community response to drought-associated changes in vegetation community. Mycologia 107, 1089-1104.

Díez, B., Pedrós-Alió, C., Marsh, T.L., Massana, R., 2001. Application of denaturing gradient gel electrophoresis (DGGE) to study the diversity of marine picoeukaryotic assemblages and comparison of DGGE with other molecular techniques. Applied and Environmental Microbiology 67, 2942-2951.

Duddridge, J., Malibari, A., Read, D., 1980. Structure and function of mycorrhizal rhizomorphs with special reference to their role in water transport. Nature 287, 834-836.

Faber, B.A., Zasoski, R.J., Munns, D.N., Shackel, K., 1991. A method for measuring hyphal nutrient and water uptake in mycorrhizal plants. Canadian Journal of Botany 69, 87-94.

Falagán, C., Johnson, D.B., 2014. *Acidibacter ferrireducens* gen. nov., sp. nov.: an acidophilic ferric iron-reducing gammaproteobacterium. Extremophiles 18, 1067-1073.

Fernandez, C.W., Langley, J.A., Chapman, S., McCormack, M.L., Koide, R.T., 2016. The decomposition of ectomycorrhizal fungal necromass. Soil Biology and Biochemistry 93, 38-49.

Fierer, N., Jackson, R.B., 2006. The diversity and biogeography of soil bacterial communities. Proceedings of the National Academy of Sciences of the United States of America 103, 626-631.

Frey-Klett, P., Garbaye, J.a., Tarkka, M., 2007. The mycorrhiza helper bacteria revisited. New Phytologist 176, 22-36.

Frey, P., Frey-Klett, P., Garbaye, J., Berge, O., Heulin, T., 1997. Metabolic and genotypic fingerprinting of fluorescent pseudomonads associated with the Douglas fir-*Laccaria bicolor* mycorrhizosphere. Applied and Environmental Microbiology 63, 1852-1860.

Fukuchi, S., Obase, K., Tamai, Y., Yajima, T., Miyamoto, T., 2011. Vegetation and colonization status of mycorrhizal and endophytic fungi in plant species on acidic barren at crater basin of volcano Esan in Hokkaido, Japan. Eurasian Journal of Forest Research 14, 1-11.

Fukuzawa, K., Shibata, H., Takagi, K., Satoh, F., Koike, T., Sasa, K., 2015. Roles of dominant understory *Sasa* bamboo in carbon and nitrogen dynamics following canopy tree removal in a cool-temperate forest in northern Japan. Plant Species Biology 30, 104-115.

Garcia, K., Delaux, P.M., Cope, K.R., Ané, J.M., 2015. Molecular signals required for the establishment and maintenance of ectomycorrhizal symbioses. New Phytologist 208, 79-87.

Gordon, G.J., Gehring, C.A., 2011. Molecular characterization of pezizalean ectomycorrhizas associated with pinyon pine during drought. Mycorrhiza 21, 431-441.

Hanning, I.B., Ricke, S.C., 2011. Prescreening of microbial populations for the assessment of sequencing potential. High-throughput next generation sequencing: methods and applications, 159-170.

Hansen, K., Pfister, D.H., 2006. Systematics of the Pezizomycetes—the operculate discomycetes. Mycologia 98, 1029-1040.

Herlemann, D.P., Labrenz, M., Jürgens, K., Bertilsson, S., Waniek, J.J., Andersson, A.F., 2011. Transitions in bacterial communities along the 2000 km salinity gradient of the Baltic Sea. The ISME journal 5, 1571-1579.

Hernandez, J.A.C., Šebesta, J., Kopecky, L., Landaverde, R.L., 2014. Application of geomorphologic knowledge for erosion hazard mapping. Natural Hazards 71, 1323-1354.

Heuer, H., Krsek, M., Baker, P., Smalla, K., Wellington, E., 1997. Analysis of actinomycete communities by specific amplification of genes encoding 16S rRNA and gel-electrophoretic separation in denaturing gradients. Applied and Environmental Microbiology 63, 3233-3241.

Holec, J., Wild, J., 2011. Fungal diversity in sandstone gorges of the Bohemian Switzerland National Park (Czech Republic): impact of climatic inversion. Czech Mycol 63, 243-263.

Hong, C., Si, Y., Xing, Y., Li, Y., 2015. Illumina MiSeq sequencing investigation on the contrasting soil bacterial community structures in different iron mining areas. Environmental Science and Pollution Research, 1-12.

Hubbell, S., 2001. The unified neutral theory of biodiversity and biogeography. Princeton University Press Princeton.

Ishaq, S.L., Johnson, S.P., Miller, Z.J., Lehnhoff, E.A., Olivo, S., Yeoman, C.J., Menalled, F.D., 2017. Impact of cropping systems, soil inoculum, and plant species identity on soil bacterial community structure. Microbial Ecology 73, 417-434.

Ishii, H.T., Kobayashi, T., Uemura, S., Takahashi, K., Hanba, Y.T., Sumida, A., Hara, T., 2008. Removal of understory dwarf bamboo (*Sasa kurilensis*) induces changes in water-relations characteristics of overstory *Betula ermanii* trees. Journal of Forest Research 13, 101-109.

Keeney, D.R., Nelson, D., 1982. Nitrogen-inorganic forms, In: Page, A.L. (Ed.), Methods of soil analysis-Part 2. Chemical and microbiological properties, 2nd ed. American Society of Agronomy, Madison, pp. 643-698.

Kruskal, W.H., Wallis, W.A., 1952. Use of ranks in one-criterion variance analysis. Journal of the American Statistical Association 47, 583-621.

Kudoh, H., Kadomatsu, M., Noda, M., Akibayashi, Y., Natsume, S., Kaneko, K., 1999. Long-term observation on the growth of *Sasa kurilensis* regenerated after mass flowering and associated plants in northern Japan: a 31 year-observation. Research Bulletins of the College Experiment Forests-Hokkaido University (Japan) 56, 30-40.

Lexa, J., Sebesta, J., Chávez, J.A., Hernández, W., Pecskay, Z., 2011. Geology and volcanic evolution in the southern part of the San Salvador Metropolitan Area. Journal of Geosciences 56, 106-140.

Li, W., Fu, L., Niu, B., Wu, S., Wooley, J., 2012. Ultrafast clustering algorithms for metagenomic sequence analysis. Briefings in Bioinformatics 13, 656-668.

Lindahl, B.D., De Boer, W., Finlay, R.D., 2010. Disruption of root carbon transport into forest humus stimulates fungal opportunists at the expense of mycorrhizal fungi. The ISME journal 4, 872-881.

Lladó, S., López-Mondéjar, R., Baldrian, P., 2017. Forest soil bacteria: diversity, involvement in ecosystem processes, and response to global change. Microbiology and Molecular Biology Reviews 81, e00063-00016.

Magoč, T., Salzberg, S.L., 2011. FLASH: fast length adjustment of short reads to improve genome assemblies. Bioinformatics 27, 2957-2963.

Makita, A., 1992. Survivorship of a monocarpic bamboo grass, *Sasa kurilensis*, during the early regeneration process after mass flowering. Ecological Research 7, 245-254.

Makita, A., 1998. The significance of the mode of clonal growth in the life history of bamboos. Plant Species Biology 13, 85-92.

Makita, A., Konno, Y., Fujita, N., Hamabata, E., 1993. Recovery of a *Sasa tsuboiana* population after mass flowering and death. Ecological Research 8, 215-224.

Marschner, H., Dell, B., 1994. Nutrient uptake in mycorrhizal symbiosis. Plant and Soil 159, 89-102.

May, L.A., Smiley, B., Schmidt, M.G., 2001. Comparative denaturing gradient gel electrophoresis analysis of fungal communities associated with whole plant corn silage. Canadian Journal of Microbiology 47, 829-841.

McKinley, V., Peacock, A., White, D., 2005. Microbial community PLFA and PHB responses to ecosystem restoration in tallgrass prairie soils. Soil Biology and Biochemistry 37, 1946-1958.

Muyzer, G., De Waal, E.C., Uitterlinden, A.G., 1993. Profiling of complex microbial populations by denaturing gradient gel electrophoresis analysis of polymerase chain reaction-amplified genes coding for 16S rRNA. Applied and Environmental Microbiology 59, 695-700.

Muyzer, G., Smalla, K., 1998. Application of denaturing gradient gel electrophoresis (DGGE) and temperature gradient gel electrophoresis (TGGE) in microbial ecology. Antonie van Leeuwenhoek 73, 127-141.

Nagendra, H., 2002. Opposite trends in response for the Shannon and Simpson indices of landscape diversity. Applied Geography 22, 175-186.

Nakashizuka, T., 1988. Regeneration of beech (*Fagus crenata*) after the simultaneous death of undergrowing dwarf bamboo (*Sasa kurilensis*). Ecological Research 3, 21-35.

Nguyen, N.-L., Kim, Y.-J., Hoang, V.-A., Subramaniyam, S., Kang, J.-P., Kang, C.H., Yang, D.-C., 2016. Bacterial Diversity and Community Structure in Korean Ginseng Field Soil Are Shifted by Cultivation Time. Plos One 11, e0155055.

Ofek, M., Hadar, Y., Minz, D., 2012. Ecology of root colonizing Massilia (*Oxalobacteraceae*). Plos One 7, e40117.

Oliveira, R.S., Franco, A.R., Castro, P.M., 2012. Combined use of *Pinus pinaster* plus and inoculation with selected ectomycorrhizal fungi as an ecotechnology to improve plant performance. Ecological Engineering 43, 95-103.

Oshima, Y., 1962. Ecological studies of *Sasa* communities. V. Influence of light intensity, snow depth and temperature upon the development of *Sasa kurilensis* community. Bot Mag Tokyo 75, 43-48.

Osman, K.T., 2013. Forest soils: properties and management. Springer, Heidelberg.

Post, W.M., Emanuel, W.R., Zinke, P.J., Stangenberger, A.G., 1982. Soil carbon pools and world life zones. Nature 298, 156-159.

Pylro, V.S., Roesch, L.F.W., Morais, D.K., Clark, I.M., Hirsch, P.R., Tótola, M.R., 2014. Data analysis for 16S microbial profiling from different benchtop sequencing platforms. Journal of Microbiological Methods 107, 30-37.

R Core Team, 2015. R: A language and environment for statistical computing. R Foundation for Statistical Computing, Vienna, Austria.

Rapidel, B., 2011. Ecosystem services from agriculture and agroforestry: measurement and payment. Routledge.

Schüßler, A., Martin, H., Cohen, D., Fitz, M., Wipf, D., 2006. Characterization of a carbohydrate transporter from symbiotic glomeromycotan fungi. Nature 444, 933-936.

Schimel, J., 1995. Ecosystem consequences of microbial diversity and community structure. Springer.

Schmidt, P.-A., Bálint, M., Greshake, B., Bandow, C., Römbke, J., Schmitt, I., 2013. Illumina metabarcoding of a soil fungal community. Soil Biology and Biochemistry 65, 128-132.

Simpson, E.H., 1949. Measurement of diversity. Nature 163, 688.

Suyama, Y., Obayashi, K., Hayashi, I., 2000. Clonal structure in a dwarf bamboo (*Sasa senanensis*) population inferred from amplified fragment length polymorphism (AFLP) fingerprints. Molecular Ecology 9, 901-906.

Takahashi, K., Uemura, S., Suzuki, J.I., Hara, T., 2003. Effects of understory dwarf bamboo on soil water and the growth of overstory trees in a dense secondary *Betula ermanii* forest, northern Japan. Ecological Research 18, 767-774.

Tedersoo, L., Kõljalg, U., Hallenberg, N., Larsson, K.H., 2003. Fine scale distribution of ectomycorrhizal fungi and roots across substrate layers including coarse woody debris in a mixed forest. New Phytologist 159, 153-165.

Ter Braak, C.J., Smilauer, P., 2002. CANOCO reference manual and CanoDraw for Windows user's guide: software for canonical community ordination (version 4.5).

Toyooka, H., Sato, M., Ishizuka, S., 1983. Distribution map of the Sasa group in Hokkaido, Explanatory note. Forestry and Forest Products Research Institute, Hokkaido Branch, Sapporo.

Tripathi, S.K., Sumida, A., Ono, K., Shibata, H., Uemura, S., Takahashi, K., Hara, T., 2006. The effects of understorey dwarf bamboo (*Sasa kurilensis*) removal on soil fertility in a *Betula ermanii* forest of northern Japan. Ecological Research 21, 315-320.

Tripathi, S.K., Sumida, A., Shibata, H., Uemura, S., Ono, K., Hara, T., 2005. Growth and substrate quality of fine root and soil nitrogen availability in a young *Betula ermanii* forest of northern Japan: effects of the removal of understory dwarf bamboo (*Sasa kurilensis*). Forest Ecology and Management 212, 278-290.

Tsutsumi, M., Kojima, H., Uemura, S., Ono, K., Sumida, A., Hara, T., Fukui, M., 2009. Structure and activity of soil-inhabiting methanotrophic communities in northern forest of Japan. Soil Biology and Biochemistry 41, 403-408.

Uroz, S., Ioannidis, P., Lengelle, J., Cébron, A., Morin, E., Buée, M., Martin, F., 2013. Functional assays and metagenomic analyses reveals differences between the microbial communities inhabiting the soil horizons of a Norway spruce plantation. Plos One 8, e55929.

Van Der Heijden, M.G., Bardgett, R.D., Van Straalen, N.M., 2008. The unseen majority: soil microbes as drivers of plant diversity and productivity in terrestrial ecosystems. Ecology Letters 11, 296-310.

Vishniac, H.S., 2006. A multivariate analysis of soil yeasts isolated from a latitudinal gradient. Microbial Ecology 52, 90-103.

Wang, Y., Sheng, H.-F., He, Y., Wu, J.-Y., Jiang, Y.-X., Tam, N.F.-Y., Zhou, H.-W., 2012. Comparison of the levels of bacterial diversity in freshwater, intertidal wetland, and marine sediments by using millions of illumina tags. Applied and Environmental Microbiology 78, 8264-8271.

Appendices

Table S1. Differences in DNA concentration between the SI and SR plots.

Plot	Date	Circle	Conc.(ng/µl)	Plot	Date	Circle	Conc.(ng/µl)
SI	23 Jul 2014	1	28.351	SR	23 Jul 2014	1	46.861
		2	40.447			2	45.573
		3	17.813			3	27.711
	1 Oct 2014	1	10.129		1 Oct 2014	1	9.601
		2	14.091			2	21.686
		3	24.38			3	17.675
	3 Jun 2015	1	9.096		3 Jun 2015	1	17.717
		2	24.447			2	14.723
		3	13.811			3	31.851
	4 Aug 2015	1	33.711		4 Aug 2015	1	44.971
		2	40.915			2	26.911
		3	29.245			3	22.291
	1 Oct 2015	1	24.203		1 Oct 2015	1	36.731
		2	31.587			2	19.66
		3	29.352			3	33.982

Table S2. Raw data statistics of bacterial communities

Plot	Date	Circle	Total Bases	Read Count	GC (%)	AT (%)	Q20 (%)	Q30 (%)
		1	106,813,788	358,224	56.25	43.75	81.96	70.62
	23 Jul 2014	2	85,320,601	285,168	55.86	44.14	82.16	70.88
		3	110,351,379	370,626	55.72	44.28	82.18	70.96
		1	113,504,386	379,528	56.42	43.58	81.96	70.64
	1 Oct 2014	2	88,661,898	296,292	56.54	43.46	81.89	70.53
		3	112,564,829	375,830	56.67	43.33	81.8	70.41
		1	100,104,005	335,226	56.11	43.89	81.91	70.54
SI	3 Jun 2015	2	86,162,617	288,204	55.76	44.24	82.09	70.73
		3	88,220,582	295,218	56.14	43.87	80.56	68.72
		1	85,650,991	285,820	56.31	43.69	82.3	71.02
	4 Aug 2015	2	73,492,083	245,118	56.25	43.75	82.17	70.9
		3	89,015,644	297,088	56.17	43.83	81.53	70.07
		1	128,592,086	429,738	56.54	43.46	80.79	68.96
	1 Oct 2015	2	112,279,352	375,324	56.15	43.85	82.58	71.4
		3	144,223,433	482,580	56.12	43.88	81.92	70.47
		1	89,938,656	300,364	57.1	42.9	81.96	70.62
SR	23 Jul 2014	2	107,242,042	358,364	56.91	43.09	82.39	71.24
		3	94,192,006	314,838	57.07	42.93	81.71	70.31

	1	113,419,053	379,704	56.46	43.54	81.65	70.27
1 Oct 2014	2	85,372,011	284,914	56.36	43.64	81.43	69.83
	3	102,593,387	344,590	55.91	44.1	81.89	70.51
	1	96,801,019	324,266	56.1	43.9	82.15	70.88
3 Jun 2015	2	86,778,912	291,682	55.57	44.43	82.56	71.37
	3	90,386,590	301,414	56.6	43.4	81.49	70
	1	90,420,735	301,746	56.63	43.37	81.73	70.32
4 Aug 2015	2	84,443,384	281,760	56.23	43.78	82.21	70.92
	3	130,731,752	437,250	56.57	43.43	82.23	71.03
	1	99,812,900	334,104	56.55	43.45	82.61	71.36
1 Oct 2015	2	122,715,114	410,278	56.05	43.95	82.94	71.83
	3	116,386,825	389,094	56.57	43.44	82.04	70.65

Table S3. Raw data statistics of fungal communities

Plot	Date	Circle	Total Bases	Read Count	GC (%)	AT (%)	Q20 (%)	Q30 (%)
		1	107,626,875	390,378	47.04	52.96	80.74	70.1
	23 Jul 2014	2	110,425,124	418,320	45.4	54.6	80.5	69.94
		3	90,119,085	315,072	46.65	53.35	80.87	70.01
		1	104,649,168	396,936	45.44	54.57	80.03	69.46
	1 Oct 2014	2	110,971,544	393,556	46.71	53.29	81.25	70.55
		3	87,656,732	300,360	41.13	58.87	82.45	71.42
		1	101,332,170	355,334	45.69	54.31	81.41	70.79
SI	3 Jun 2015	2	103,133,562	361,372	46.9	53.1	80.91	70.27
		3	81,459,273	283,910	47	53	81.48	70.72
		1	106,245,608	355,132	44.81	55.19	81.67	70.77
	4 Aug 2015	2	100,679,119	409,722	46.19	53.81	80.13	69.88
		3	84,575,748	301,624	45.28	54.72	81.61	70.89
		1	101,736,403	395,044	47.61	52.39	79.02	68.66
	1 Oct 2015	2	113,489,478	428,786	48.59	51.41	79.71	69.18
		3	112,427,984	412,190	47.26	52.74	80.41	69.83
		1	95,230,526	354,846	48.86	51.14	80.04	69.4
SR	23 Jul 2014	2	113,079,032	431,036	45.05	54.95	80.13	69.62
		3	102,261,210	395,556	42.81	57.19	81.06	70.44

	1	106,185,540	386,746	47.76	52.24	80.6	70.02
1 Oct 2014	2	97,470,169	398,146	46.39	53.61	78.79	68.66
	3	98,227,541	363,596	47.35	52.65	80.91	70.3
	1	81,597,014	290,726	47.11	52.89	81.43	70.65
3 Jun 2015	2	117,989,094	407,054	47.44	52.56	81.82	71.35
	3	99,236,068	348,966	46.23	53.77	81.43	70.61
	1	109,983,382	385,106	47.7	52.3	81.08	70.39
4 Aug 2015	2	109,784,983	385,648	45.17	54.83	81.57	70.95
	3	141,399,713	534,424	47.18	52.82	80.72	70.19
	1	100,572,376	385,626	48.18	51.82	80.12	69.66
1 Oct 2015	2	90,096,435	327,090	45.05	54.96	80.9	70.42
	3	108,939,874	386,492	46.06	53.94	81.64	70.98

Table S4. Differences in the relative abundance of microbial communities between the SI and SR plots based on Kruskal-Wallis test. Significance at the $p<0.05$ level is shown in bold.

		Df	Chi-squared	*p*
Bacterial phyla				
	Acidobacteria	*1*	0.65	0.42
	Proteobacteria	*1*	4.05	**<0.05**
	Bacteroidetes	*1*	0.19	0.66
	Verrucomicrobia	*1*	0.19	0.66
	Firmicutes	*1*	0.03	0.85
	Planctomycetes	*1*	10.07	**<0.01**
	Actinobacteria	*1*	4.13	**0.04**
Proteobacteria Genera				
	Acidibacter	*1*	5.77	**0.02**
	Rhizomicrobium	*1*	3.94	**<0.05**
	Bradyrhizobium	*1*	0.10	0.76
	Burkholderia	*1*	0.01	0.92
	Sorangium	*1*	0.27	0.60
	Reyranella	*1*	1.85	0.17
	Helicobacter	*1*	0.01	0.92
	Rhodanobacter	*1*	0.70	0.40
	Pseudomonas	*1*	1.62	0.20
	Massilia	*1*	4.10	**<0.05**
	Collimonas	*1*	2.16	0.14
	Variovorax	*1*	1.62	0.20
Planctomycetes Genera				
	Gemmata	*1*	0.40	0.53
	Isosphaera	*1*	1.84	0.17
	Pirellula	*1*	0.30	0.58
	Planctomyces	*1*	0.04	0.83

	Rhodopirellula	*1*	0	1
	Schlesneria	*1*	0.42	0.52
	Singulisphaera	*1*	0.93	0.34
Actinobacteria Genera				
	Catenulispora	*1*	0.18	0.67
	Mycobacterium	*1*	3.15	0.08
	Acidothermus	*1*	1.85	0.17
	Sporichthya	*1*	6.00	**0.01**
	Salinibacterium	*1*	2.65	0.10
	Marmoricola	*1*	1	0.32
	Propionibacterium	*1*	0.01	0.91
	Kutzneria	*1*	1	0.32
	Longimycelium	*1*	0.48	0.49
	Kitasatospora	*1*	0	1
	Iamia	*1*	2.25	0.13
	Enterorhabdus	*1*	0.01	0.91
Fungal phyla				
	Ascomycota	*1*	14.5	**<0.001**
	Basidiomycota	*1*	0.41	0.52
	Zygomycota	*1*	0.02	0.89
Fungal classes				
	Pezizomycetes	*1*	7.77	**<0.01**
	Saccharomycetes	*1*	0.83	0.36
	Agaricomycetes	*1*	0.01	0.92
	Tremellomycetes	1	11.46	**<0.001**
	Wallemiomycetes	1	<0.001	0.98
Fungal families				
	Pezizaceae	1	6.82	**<0.01**
	Mortierellaceae	1	0.27	0.60
	Tricholomataceae	1	1.84	0.17
	Russulaceae	1	0.10	0.75

Sebacinaceae	1	6.86	**<0.01**
Thelephoraceae	1	1.32	0.25
Filobasidiaceae	1	6.82	**<0.01**
Hydnaceae	1	0.27	0.60
Clavariaceae	1	0.01	0.92
Saccharomycodaceae	1	0.88	0.35
Mycenaceae	1	0.10	0.75
Paxillaceae	1	0.88	0.35
Ceratobasidiaceae	1	0.27	0.60
Clavulinaceae	1	0.53	0.46
Incertae sedis	1	5.91	**0.02**
Geminibasidiaceae	1	4.81	**0.03**
Lobulomycetaceae	1	0.04	0.83

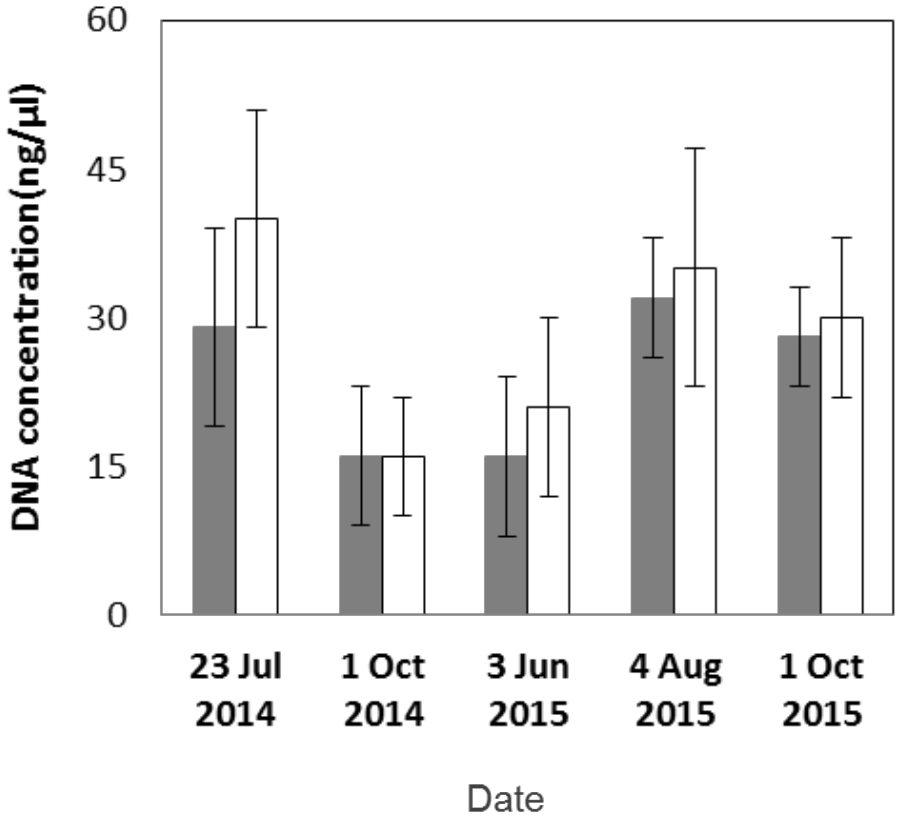

Fig. S1. Differences in DNA concentration between the SI (gray) and SR (white) plots. Vertical lines indicate standard errors (*n*=15).

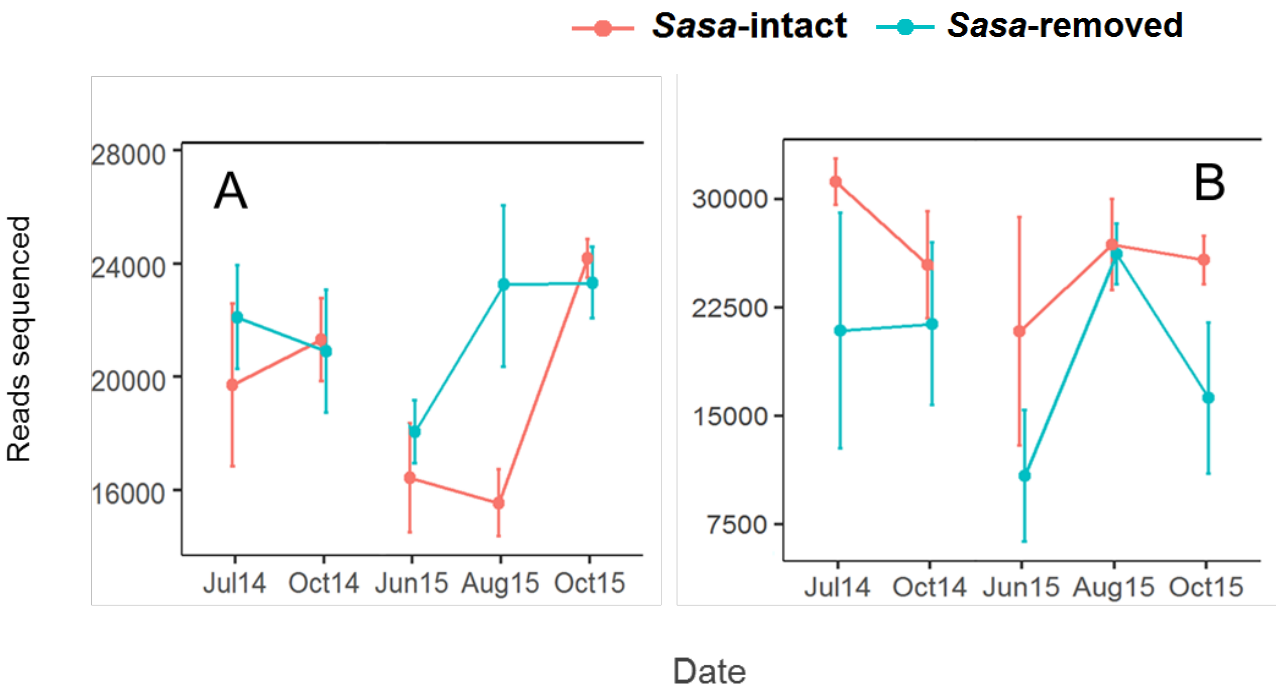

Fig. S2. The abundance of total bacteria (A) and fungi (B) between the SI and SR plots for the five sampling dates (*n*=3).